British Journal of Pharmacology

DOI:10.1111/j.1476-5381.2010.00988.x
www.brjpharmacol.org

Themed Section: Imaging – the Interface with Pharmacology

REVIEW

Imaging calcium signals *in vivo*: a powerful tool in physiology and pharmacology

James T Russell

Section on Cell Biology and Signal Transduction, NICHD, NIH, Bethesda, MD, USA

Correspondence
Dr James T Russell, Laboratory of Cellular and Molecular Neurophysiology, NICHD, NIH, Bldg. 49, Room 5A-22, 49 Convent Drive, MSC 4480, Bethesda, MD 20892-4480, USA.
E-mail: james@helix.nih.gov

Keywords
calcium imaging; *in vivo* imaging; calcium indicators

Received
21 May 2010
Revised
9 July 2010
Accepted
29 July 2010

The design and engineering of organic fluorescent Ca^{2+} indicators approximately 30 years ago opened the door for imaging cellular Ca^{2+} signals with a high degree of temporal and spatial resolution. Over this time, Ca^{2+} imaging has revolutionized our approaches for tissue-level spatiotemporal analysis of functional organization and has matured into a powerful tool for *in situ* imaging of cellular activity in the living animal. *In vivo* Ca^{2+} imaging with temporal resolution at the millisecond range and spatial resolution at micrometer range has been achieved through novel designs of Ca^{2+} sensors, development of modern microscopes and powerful imaging techniques such as two-photon microscopy. Imaging Ca^{2+} signals in ensembles of cells within tissue in 3D allows for analysis of integrated cellular function, which, in the case of the brain, enables recording activity patterns in local circuits. The recent development of miniaturized compact, fibre-optic-based, mechanically flexible microendoscopes capable of two-photon microscopy opens the door for imaging activity in awake, behaving animals. This development is poised to open a new chapter in physiological experiments and for pharmacological approaches in the development of novel therapies.

LINKED ARTICLES
This article is part of a themed section on Imaging. To view the other articles in this section visit http://dx.doi.org/10.1111/bph.2011.163.issue-8 *BJP* has previously published an *Imaging in Pharmacology* themed section, edited by A Davenport and C Daly. To view this section visit http://dx.doi.org/10.1111/bph.2010.159.issue-4

Abbreviations
BRET, bioluminescence resonance energy transfer; CFP, cyan fluorescent protein; FPI, fluorescent protein indicators; FRET, foster resonance energy transfer; GFP, green fluorescent protein; YFP, yellow fluorescent protein

Introduction

Ca^{2+} is an ubiquitous intracellular messenger that regulates multiple cellular functions such as secretion, contraction, cellular excitability and gene expression in all organ systems. The earliest recognition that calcium ions are essential for regulating biological processes was by Sydney Ringer, who serendipitously found that 'lime salt' is necessary to maintain the contractions of an isolated frog heart (Ringer, 1883). Integrated function of organ systems in general is achieved by concerted signalling by entire cellular ensembles in organs in synchronous and/or asynchronous modes, and Ca^{2+} ions play a central role in such signalling. Therefore, understanding Ca^{2+} signals, and their temporal and spatial characteristics in cells and tissues is crucial to both gain knowledge of the physiological regulation of the organ system, and for developing pharmacological approaches. The pioneering chemical synthesis of organic Ca^{2+} indicators based on the Ca^{2+} chelating properties of EGTA in the 1970s by Roger Tsien and colleagues, made direct monitoring of cellular Ca^{2+} signals possible (Tsien, 1980; 1981; Grynkiewicz *et al.*, 1985). Early studies focused on measuring Ca^{2+} signals in acutely isolated living cells and cells in tissue culture. It is however necessary to understand the signal flow between cells

in intact systems, and characterize the spatially discrete and temporally complex signalling in order to describe systems level physiological regulation. Since many physiological signalling scenarios cannot be accurately reproduced *in vitro*, it is essential to record and analyse integrated signals between cells in living tissue *in vivo*. Advances in optical and computing technologies yielded powerful microscope systems that enabled the realization of this goal. By combining appropriate Ca^{2+} indicators with appropriate optical imaging techniques, cellular Ca^{2+} signals and sometimes fluxes have been monitored with a high degree of spatial and temporal resolution. Such imaging approaches have been developed for a number of tissues and organ systems in various animal models, and in the last decade, this effort has led to breathtaking insights into signalling in intact systems, and have been reviewed extensively (Garaschuk *et al.*, 2007; Paredes *et al.*, 2008; Rochefort *et al.*, 2008). In this review I present recent technical developments in the fields of Ca^{2+} indicators and *in vivo* Ca^{2+} imaging. These technical advances have made Ca^{2+} imaging a powerful approach for functional and pharmacological studies *in vivo*.

In vivo calcium imaging – an overview

Imaging Ca^{2+} signals in cells in culture and tissue slices became routine in most laboratories over the last two decades. During this time, methods were developed to investigate the cellular physiology and pharmacology of Ca^{2+} signals in many different cellular and tissue systems in different animal models (see for review Bootman and Berridge, 1995). Most initial studies were restricted to imaging cells in culture. Very early on, however, it was recognized that cellular Ca^{2+} signals have complex spatio-temporal forms and spread as waves within cells, and in between cells. For that reason, acutely isolated tissue and organs were loaded with Ca^{2+} indicator dyes and imaged (Duffy and MacVicar, 1995; Porter and McCarthy, 1995). An alternative preparation for brain tissue studies is the use of organotypic cultures of brain slice preparations (Dani *et al.*, 1992). Here, the brain slices are maintained in culture in an air–water interphase where the slices thinned out but retained more or less the cytoarchitecture of the original brain circuits (Gahwiler, 1981). These cultures were labelled and imaged to study physiological signalling modes (Dani *et al.*, 1992). By this time, the recognition that Ca^{2+} signals are organized in specialized signalling microdomains in cells and coordinated in specific temporal sequences led to experiments using more intact systems.

Ideally, it is necessary to image organ systems in the living animal to gain understanding of signalling patterns within tissue. In experiments with liver cells in culture and perfused intact livers, it was found that agonist-evoked Ca^{2+} signals were qualitatively and quantitatively different in the intact preparation compared with those in isolated hepatocytes (Gaspers and Thomas, 2005). The brain is unique in its signal organization, where sensations and behaviours are encoded in patterns of activity in neuronal networks. Through a sequence of network, activity information is relayed to other associative brain regions where signal integration and activity patterns are achieved. This chain of events perhaps occurs in a series of important processing steps in local microcircuits. Activity in local circuits is not accurately recorded in isolated brain slice or culture preparations. It is necessary to image intact brain circuits in the living animal in order to understand the cellular signalling in physiology and information processing. In addition, a number of studies have shown that dendritic excitability is modulated by various factors including ionic composition, excitatory and inhibitory inputs, and activation and inactivation of voltage-dependent conductances. For that reason, dendritic signals recorded in brain slice preparations are different from *in situ* recordings in intact animals (Svoboda *et al.*, 1999). These observations provided the impetus for the development of methods to discretely deliver Ca^{2+} indicators to cells *in situ* either using cell injection or bulk loading for imaging in the intact living animal.

Thus, it is only more recently that live animals were imaged to investigate physiological signalling in intact organ systems *in vivo*. The earliest experiments were carried out in invertebrates, worms and insects, plants, and small vertebrates, for example, zebrafish (Friedrich and Korsching, 1997; Dal Santo *et al.*, 1999; Plieth, 2001). These initial studies used either expression of the luminescent Ca^{2+} sensor protein apoaequorin in transgenic organisms (Creton *et al.*, 1997) or bulk loading of cell permeant versions of organic fluorescent Ca^{2+} indicators such as Fura-2 and Fluo-3 (Stosiek *et al.*, 2003; Ohki *et al.*, 2006; Takano *et al.*, 2007). Luminescence signals were recorded using photomultiplier tubes, and fluorescence-based organic dyes were imaged using charge coupled device (CCD) camera systems with or without image intensification for signal enhancement. The development of more sensitive CCD sensors led to studies on sensory neural systems in non-mammalian brains, such as olfactory systems in the honeybee (Galizia *et al.*, 1999), *Drosophila* (Karunanithi *et al.*, 1997) and turtle (Wachowiak *et al.*, 2002) as well as the auditory system in the

cricket (Sobel and Tank, 1994). The choice of these readily accessible neural systems in lower animals was due to the very high light-scattering property of neural tissue, which restricted depth penetration in conventional imaging systems available at that time. In most tissues, particularly the brain, light scattering prevents the use of wide-field and confocal microscopy for imaging cells of interest located deep within tissue. The implementation of two-photon laser scanning microscopy finally allowed for deep tissue imaging in the brain (Hoogland *et al.*, 2009; Grewe *et al.*, 2010; Lutcke *et al.* 2010). A number of novel fibre-optic-based two-photon microendoscopes have been recently developed (Helmchen *et al.*, 2001; Gobel *et al.*, 2004), which makes the technique capable for both recording physiological activity *in vivo* and also for investigating pathophysiology of disease states. Indeed most *in vivo* imaging to date has been carried out in neural systems (see Helmchen and Kleinfeld, 2008; Homma *et al.*, 2009 for reviews). The development of multiphoton laser scanning microscopy, together with the design of fluorescent protein-based Ca^{2+} sensors that could be targeted to specific cell types in transgenic animal models, has made *in vivo* Ca^{2+} imaging into a powerful tool generally available to most physiologists and pharmacologists (see Rochefort *et al.*, 2008 for review). Two-photon confocal microscopy implemented on fixed stage microscopes are still too costly for many laboratories. Fibre-optic-based microendoscopes capable of two-photon microscopy have become more reasonably priced and are accessible by many investigators.

Calcium indicators

The ubiquitous nature of Ca^{2+} as an intracellular messenger encouraged scientists to search for Ca^{2+} indicators that would enable optical measurements of Ca^{2+} concentration in the cytoplasm of cells. The earliest measurements of intracellular Ca^{2+} dynamics occurred following the extraction and characterization of the Ca^{2+}-sensitive bioluminescent protein aequorin from the jellyfish, *Aequoria victoria* (Shimomura *et al.*, 1962). Aequorin extracted from jellyfish tissue was microinjected into cells to monitor rapid changes in intracellular Ca^{2+} by measuring luminescence changes (Hastings *et al.*, 1969; Baker *et al.*, 1971; Shimomura *et al.*, 1993). About this time metalochromatic dyes like murexide and arzenazo III were also used to measure intracellular ionized Ca^{2+} concentration (Jobsis and O'Connor, 1966; Dipolo *et al.*, 1976; Miledi *et al.*, 1977). Although these dyes were initially promising, the Ca^{2+}-dependent spectral changes were highly sensitive to pH fluctuations that were known to occur in cells (Russell and Martonosi, 1978). Aequorin, on the other hand, was not readily available and required microinjection into individual cells, and for that reason its use remained in the domain of few physiologists. Furthermore, aequorin is inactivated during light emission and hence its use was confined to experiments of short duration. With the design and development of organic fluorescent Ca^{2+} indicators for fluorimetric microscopy, a new field of research in cellular Ca^{2+} signalling began in earnest. Currently a large number of organic fluorescent probes, and fluorescent protein-based indicators are available for routine use. The most commonly used indicators are listed in Table 1.

Organic Ca^{2+} indicators

In the late 1970s Roger Tsien and colleagues synthesized the first organic fluorescent Ca^{2+} indicator, quin-2, which showed a remarkable increase in fluorescence emission upon binding Ca^{2+}. The K_d of Ca^{2+} binding was approximately 100 nM, which made quin-2 suitable as a cytoplasmic Ca^{2+} indicator. While it was put to extensive use for measurement of cytoplasmic Ca^{2+} concentration in living cells, quin-2 had a number of shortcomings (Tsien *et al.*, 1982; Grynkiewicz *et al.*, 1985). Tsien and his colleagues improved on this initial design and synthesized a series of similar compounds that altered their fluorescence properties upon Ca^{2+} binding with varying affinities (Tsien, 1980; 1981; Grynkiewicz *et al.*, 1985). This development sparked an explosion of research on cellular Ca^{2+} signalling and led to the development of a family of stable, brightly fluorescent Ca^{2+} indicators with a range of affinities for Ca^{2+} in physiological concentrations (see Paredes *et al.*, 2008). Ca^{2+}-sensitive dyes can be classified into two categories: single wavelength indicators and ratiometric indicators. The former exhibit significant Ca^{2+}-dependent change in fluorescence intensity without shifting their excitation or emission wavelengths. Ratiometric indictors, on the other hand, shift their peak wavelength of either excitation or emission upon binding Ca^{2+}. For that reason this class of dyes permit very accurate quantification of Ca^{2+} concentration that can be corrected for uneven dye loading, dye leaking photobleaching and changes in cell volume. Fura-2, Fluo-3, Fluo-4, calcium green-1 and Oregon green BAPTA were all of this family of organic Ca^{2+} indicators (Table 1). Methods were developed to fill cells with these organic molecules in high-enough concentrations suitable for fluorescence microscopy (Tsien, 1981) (see later). A number of laboratories developed technologies to investigate all aspects of the cell biology of Ca^{2+} signalling in different cell and organ systems.

Table 1

Most commonly used fluorimetric calcium indicators

Indicator	Species	Application/tissue studied	Labelling technique	Imaging technique	Spatial resolution	Response amplitude	References
Organic synthetic fluorescent dyes							
Fura-2	Blowfly	Visual system	Cell microinjection	Epifluorescence/CCD camera	Cellular/ subcellular	10–20%	Borst and Egelhaaf, 1992
Fura-2	Cricket	Auditory system	Cell microinjection	Epifluorescence/CCD camera	Cellular	6–20%	Sobel and Tank, 1994
Fluo-3	*C. elegans*	Apoptosis	Bulk microinjection	Confocal microscopy	Cellular	15%	Jain *et al.*, 1993
Fluo-3	*Drosophila*	Motor nerve terminals	Bulk loading	Confocal microscopy	Cellular	100–200%	Karunanithi *et al.*, 1997
Fura-2, Fluo-4, Indo-1	Mouse	Neocortex	Bulk microinjection	Two-photon microscopy	Cellular	20–50%	Stosiek *et al.*, 2003
Calcium green-1	Honeybee	Olfactory system	Bulk microinjection	Epifluorescence/CCD camera	Glomerular	2–5%	Galizia *et al.*, 1999
Calcium green-1	Zebrafish	Olfactory bulb	Bulk microinjection	Epifluorescence/CCD camera	Glomerular	5–10%	Friedrich and Korsching, 1997
Calcium green-1	Turtle	Olfactory system	Bulk loading	Epifluorescence/CCD camera	Cellular	5–20%	Wachowiak *et al.*, 2002
Oregon green BAPTA	Mouse	Neocortex	Cell microinjection	Two-photon microscopy	Cellular/ subcellular	40–200%	Helmchen *et al.*, 1999; Svoboda *et al.*, 1999
Oregon green BAPTA	Cat	Visual cortex	Bulk microinjection	Two-photon microscopy	Cellular	40–200%	Ohki *et al.*, 2006
Oregon green BAPTA	Ferrett	Visual cortex	Bulk microinjection	Two-photon microscopy	Cellular	10–30%	Shummers *et al.*, 2008
Rhod-2	Mouse	Cortical astrocytes	Bulk microinjection	Two-photon microscopy	Cellular	10–100%	Takano *et al.*, 2007
Aequorin-based luminescence calcium indicators							
Aequorin	Tobacco	Whole plant	Transgenic	Luminescence detection	Bulk tissue	NA	Knight *et al.*, 1991
Aequorin	*Arabidopsis*	Whole plant	Transgenic	Luminescence detection	Bulk tissue	~10-fold	Knight *et al.*, 1996; Liu *et al.*, 2006
Aequorin	Zebrafish	Development	mRNA injection/transgenic	Luminescence detection	Tissue/cellular	5- to 10-fold	Creton *et al.*, 1997; Cheung *et al.*, 2006
Aequorin	*Drosophila*	Brain/mushroom bodies	Transgenic	Luminescence/photon counting	Bulk tissue	>100%	Martin *et al.*, 2007
Fluorescent protein-based calcium indicators							
DsRed/inverse pericam	*C. elegans*	Pharyngeal muscles	Transgenic	Epifluorescence/CCD camera	Bulk tissue	20–30%	Shimozono *et al.*, 2004
YC 2.1, YC 3.1	*C. elegans*	Brain/sensory neurons	Transgenic	Epifluorescence/CCD camera	Bulk tissue	50–60%	Kerr *et al.*, 2000
G-CaMP	*Drosophila*	Olfactory system	Transgenic	Two-photon microscopy	Bulk cellular	100%	Wang *et al.*, 2003
YC 3.1	*Drosophila*	Flight muscle	Transgenic	Confocal microscopy	Bulk cellular	12%	Gordon and Dickinson, 2006
G-CaMP2, synapcam, YC 2.3, TN-L15	*Drosophila*	Motor neurons	Transgenic	Epifluorescence/CCD camera	Cellular	30–700%	Guerrero *et al.*, 2005; Mank *et al.*, 2006; Reiff *et al.*, 2005
YC 2.1	Zebrafish	Spinal cord/neurons	Transgenic	Confocal microscopy	Cellular	15%	Higashijima *et al.*, 2003
YC 2.12	Zebrafish	Development	Transgenic	Epifluorescence/CCD camera	Bulk cellular	NA	Tsuruwaka *et al.*, 2007
Camgaroo, inverse pericam	Mouse	Olfactory bulb/neurons	Transgenic	Epifluorescence/CCD camera	Bulk tissue	1–3%	Hasan *et al.*, 2004
G-CaMP2	Mouse	Cerebellum/neurons	Transgenic	Epifluorescence/CCD camera, two-photon microscopy	Bulk tissue	50%	Diez-Garcia *et al.*, 2007
G-CaMP2	Mouse	Heart	Transgenic	Two-photon microscopy	Bulk tissue	60–70%	Tallini *et al.*, 2006
YC 3.12	Mouse	Brain/neurons	Transgenic	Two-photon microscopy	Cellular	10–30%	Hasan *et al.*, 2004
Cer TN-L15	Mouse	Cortex/neurons	Transgenic	Two-photon microscopy	Cellular	5–10%	Heim *et al.*, 2007
Cer TN-L15	Mouse	Brain/astrocytes	Transgenic	Two-photon microscopy	Cellular	10–20%	Atkin *et al.*, 2009
YC 3.60, Cer TN -L15, G-CaMP3	*C. elegans*, mouse	Cortex/neurons	Transgenic	Two-photon microscopy	Cellular	30–500%	Tian *et al.*, 2009

C. elegans, *Caenorhabditis elegans*; CCD, charge coupled device; NA, not available.

A large number of fluorescent organic Ca^{2+} indicators became available with varying affinities towards Ca^{2+} and binding rate constants (Paredes *et al.*, 2008). The high-affinity dyes with dissociation constants in submicromolar concentrations (0.1–0.3 μM) were useful for measurements of cytoplasmic Ca^{2+} concentrations (Kao *et al.*, 1989). The low-affinity indicators with dissociation constants in hundreds of micromolar Ca^{2+} were useful for measurement of Ca^{2+} within cellular compartments where Ca^{2+} concentrations ranged in the low millimolar range (Park *et al.*, 2002). Since cytoplasmic Ca^{2+} signals are generally transient in nature, they are measured under non-equilibrium conditions. Because of that reason, it is necessary to be aware of the speed with which an indicator binds Ca^{2+}. Most commonly used organic fluorescent Ca^{2+} indicators have equilibrium binding rate constants between 5 and 20 μs. To date, there are more than 25 different organic fluorescent dyes that are commercially available from different sources. These dyes vary widely in their Ca^{2+}-binding affinity and binding time constants (see Paredes *et al.*, 2008 for review; see also Invitrogen).

Fluorescent protein-based Ca^{2+} indicators (FPIs)

The discovery of fluorescent proteins occurring in nature resulted in the widespread use of green fluorescent protein (GFP) in cell biological research (Tsien, 1998). FPIs are Ca^{2+}-sensitive fluorescent or luminescent proteins and their chimeric constructs that can be expressed in specific subsets of cells in the tissue under investigation, by the use of cell and tissue specific promoters (Miyawaki *et al.*, 1997; Hasan *et al.*, 2004; Rogers *et al.*, 2005; Heim *et al.*, 2007). Once the codons were humanized, these proteins were genetically targeted and expressed in specific cells and cellular compartments non-invasively using molecular biology and transgenic techniques. Mutant forms of these fluorescent proteins were designed with widely differing spectral emission properties (Heim *et al.*, 1994; Cubitt *et al.*, 1995), and this opened the possibility for developing fluorescent proteins with Ca^{2+}-induced Foster resonance energy transfer (FRET) properties (Miyawaki *et al.*, 1997; 1999; Heim *et al.*, 2007). Chimeric constructs of fluorescent proteins and Ca^{2+}-binding proteins such as calmodulin and troponin-C were engineered yielding cell targetable Ca^{2+} indicators. Some of these new generation fluorescent protein Ca^{2+} indicators (FPIs) were designed with two different GFP mutants [e.g. cyan fluorescent protein (CFP) and yellow fluorescent protein (YFP)] based on changes in FRET efficiency upon Ca^{2+} binding. FPIs are a powerful tool for *in vivo* Ca^{2+} imaging, since they support detection of signals within cells and cellular compartments from discrete cell types in intact tissue. This has been the holy grail for the field, particularly in the nervous system, where using this technique, local network activity can be monitored in a physiologically behaving animal with appropriate techniques.

During the 1990s, two classes of genetically encodable Ca^{2+} indicators became available, those based on fluorescent proteins, for example, cameleons (Miyawaki *et al.*, 1997; 1999; Heim *et al.*, 2007; see also Tian *et al.*, 2009), and those based on luminescent proteins, aequorin and obelin (Illarionov *et al.*, 1995; Martin *et al.*, 2007; Tian *et al.*, 2009). The very first of the genetically encoded Ca^{2+} sensors were different subclasses of circularly permuted GFP, where mutating different amino acids near the chromophore portion of GFP yielded indicators that reversibly changed fluorescence intensity when the ambient Ca^{2+} concentration changed. These were the pericams that increased fluorescence intensity with increasing Ca^{2+} concentration and inverse pericams that decreased fluorescence intensity with increasing Ca^{2+} concentration and ratiometric pericams (Nagai *et al.*, 2001). Pericams have been successfully used in many physiological imaging applications from *Caenorhabditis elegans* muscle contraction to mouse neurons (Robert *et al.*, 2001; Hasan *et al.*, 2004; Shimozono *et al.*, 2004). The second class of fluorescent protein Ca^{2+} indicators were camgaroos, and they were designed with the Ca^{2+}-binding protein calmodulin inserted between positions 144 and 146 of YFP. Ca^{2+}-dependent conformational change in the calmodulin moiety induces ionization of the chromophore resulting in a seven- to eightfold increase in YFP fluorescence (Baird *et al.*, 1999). Camgaroos, like pericams, have proven to be useful for physiological recording *in vivo* in *Drosophila* and mice, where activity in olfactory bulb neurons was recorded (Hasan *et al.*, 2004). The third iteration of circularly permuted GFP was G-CaMP, and this new design resulted in a large increase in GFP fluorescence upon Ca^{2+} binding (Nakai *et al.*, 2001). G-CaMP produced much greater fluorescence changes in response to increases in Ca^{2+} concentration compared with the FRET-based designs, and were quickly adopted to monitor Ca^{2+} signals *in vivo* in a number of species (Wang *et al.*, 2003; Pologruto *et al.*, 2004). Although G-CaMP's slow kinetics limited the temporal resolution of signals, the extraordinary brightness and therefore the increased signal-to-noise were attractive. A number of improvements were made by point mutation strategies resulting in G-CaMP2 and, more recently, G-CaMP3 with improved kinetics (Chaigneau *et al.*, 2007; He *et al.*, 2008; Hoogland *et al.*, 2009). G-CaMP3 is the most recent

development and has at least a threefold increased brightness and dynamic range making it potentially a very valuable tool for *in vivo* imaging (Tian *et al.*, 2009). G-CaMP3 was used for high-speed imaging of network activity in the motor cortex, and detected Ca^{2+} transient amplitudes linearly dependent on action potential number (Tian *et al.*, 2009).

Using mutated GFP variants, cameleons, a new class of chimeric constructs were designed, which produce Ca^{2+}-dependent FRET between the two fluorescent proteins in the chimera of CFP and YFP/Venus (Miyawaki *et al.*, 1999) or cerulean and citrine (Griesbeck *et al.*, 2001). Calmodulin or troponin-C served as the Ca^{2+}-sensitive domains in the construct which underwent conformational change leading to increased FRET efficiency. A number of different indicators of this class were synthesized including YC 2.1, YC 3.1, YC 3.60 (Miyawaki *et al.*, 1997; Hasan *et al.*, 2004; Nagai *et al.*, 2004; Reiff *et al.*, 2005) and troponin-C-based indicators such as CerTN-L15, and TN-XXL (Reiff *et al.*, 2005; Heim *et al.*, 2007; Mank *et al.*, 2008). Many of these FRET-based cameleons have been successfully used to record Ca^{2+} signals in different animal models *in vivo*, including *C. elegans* pharyngeal muscle (Kerr *et al.*, 2000), *Drosophila* flight muscle (Gordon and Dickinson, 2006) and in rodents (Hendel *et al.*, 2008; Atkin *et al.*, 2009). Table 1 lists the most commonly used fluorescent protein Ca^{2+} indicators for *in vivo* Ca^{2+} imaging.

The most recent development in the class of genetically encodable FPIs is the design of a chimeric construct of aequorin, the luminescent Ca^{2+} sensor, and GFP. Aequorin is a bioluminescent photoprotein that emits light upon binding to Ca^{2+} (Shimomura *et al.*, 1990). This property of aequorin has been successfully used for *in vivo* Ca^{2+} imaging in the zebrafish (see Shimomura *et al.*, 1993; Creton *et al.*, 1997). The low quantum yield of apoaequorin luminescence makes it difficult to detect Ca^{2+} events with short integration times (<1 s) or with single cell resolution. In order to overcome this problem, a chimeric construct was recently designed which mimics the native protein arrangement in the jellyfish (Shimomura *et al.*, 1993), where the Ca^{2+}-sensitive aequorin luminescence produces bioluminescence resonance energy transfer (BRET) to GFP, emitting light in the visible range (509 nm) (Baubet *et al.*, 2000; Rogers *et al.*, 2005). Using this principle, aequorin-GFP chimera were engineered, and were shown to be fast responding Ca^{2+} sensors that produce bright light emission in the visible range, over a large dynamic range of Ca^{2+} concentrations (0.1 μM–1.0 mM), and are insensitive to pH in the physiological range (Rogers *et al.*, 2005; Curie *et al.*, 2007; Martin *et al.*, 2007). Compared with aequorin alone, the light emission of the chimeric construct with the optimized flexible linker region is more than 60-fold higher (Baubet *et al.*, 2000). This Ca^{2+} sensor was named GA (GFP-aequorin), and is a powerful tool for functional mapping of neuronal circuits *in vivo* (Martin, 2008). GA offers a very high contrast, high signal-to-noise emission by virtue of the fact that light is emitted in the absence of illumination, and thus autofluorescence is non-existent. This lack of autofluorescence is an asset when imaging small structures deep within tissue. Another major advantage over fluorescence is that there is no phototoxicity and or bleaching of the fluorophore. While these are significant advantages, the major drawback of the GA luminescence imaging is the poor spatial resolution compared with fluorescence-based imaging. Temporal resolution however is most often adequate even with photon accumulation by integration over time (Pozzan and Rudolf, 2009; Drobac *et al.*, 2010). A recent review compares the advantages and disadvantages of fluorescence imaging over bioluminescence imaging using GA (Martin, 2008).

The foregoing discussion illustrates the vigorous research activity in the development of tools for imaging Ca^{2+} *in vivo* with good temporal and spatial resolution. While a number of Ca^{2+} sensors have been invented which have contributed to our understanding of cellular signalling in the context of intact animals, none have proved to be the all purpose, ideal indicator. Close attention should be paid to the choice of probe and the imaging technique that will suit the experimental requirements, in order to improve data quality and reduce toxicity. Development of probes that would allow imaging deep within tissue *in vivo* will prove to be essential.

Indicator loading techniques

Synthetic Ca^{2+} indicators

Imaging Ca^{2+} signals *in vivo* requires filling the cells with appropriate amounts of a fluorescent or luminescent Ca^{2+} indicator. Organic synthetic Ca^{2+} indicators are maximally fluorescent and have their optimal Ca^{2+} binding affinities in their ionized salt forms. These ionized species of dyes however are hydrophilic and therefore are not membrane permeant, and do not enter cells. To enable loading cells with the indicator noninvasively, Tsien and colleagues developed the esterified forms of the dyes (Tsien, 1981). Acetoxymethyl (AM) ester derivatives of the dyes, by virtue of their uncharged state at physiological pH were readily permeable across the cell membrane. Once in the cytoplasm, endogenous esterases in the cell de-esterified the dye into

the charged species, making them both highly fluorescent and with high affinity to Ca^{2+} ions. De-esterified dye molecules are charged and are impermeant and therefore are trapped with the cell, thus achieving significantly higher concentrations than in the incubate. This method of loading synthetic fluorescent indicators into cells became routine for most applications. One major problem encountered in this type of cell loading is compartmentalization of dye into cellular organelles (Del Nido *et al.*, 1998). This could be controlled to some extent by carefully optimizing incubation temperature and time for each cell and tissue type.

Microinjection of Ca^{2+}-sensitive dyes was initially the method of choice, and single cells were injected with the indicator in cells in culture, in isolated tissues, as well as in intact animals (Sobel and Tank, 1994;Helmchen *et al.*, 1999; Svoboda *et al.*, 1999). While the luminescent Ca^{2+} indicator aequorin was the first compound microinjected into cells (Hastings *et al.*, 1969; Baker *et al.*, 1971), for *in vivo* imaging the synthetic fluorescent indicators were the first to be used (Sobel and Tank, 1994; Svoboda *et al.*, 1999). Single cell microinjection is an excellent choice to image cells *in vivo*, since the cells of interest can be studied with high contrast, as the neighbouring cells are not filled. The major drawback is that only one cell is recorded at a time, and recording Ca^{2+} signals within cell ensembles is most often required to understand physiological signalling within tissue. This drawback can be overcome by a variation of this technique using bulk loading of cells with cell permeant dyes or by controlled permeabilization of cells at the vicinity of dye microinjection (see Figure 1B). Electroporation has been successfully used to fill a collection of cells (10–100) with chemical dyes such as calcium green-1 and Oregon green BAPTA-1 (OGB-1) (Nagayama *et al.*, 2007). In the brain, this technique provides a powerful method for loading a local neural circuit for imaging *in vivo*. Embryonic brain cells were labelled in this manner *in utero* (Mank *et al.*, 2008; Holtmaat *et al.*, 2009).

Using cell-permeant forms of synthetic chemical Ca^{2+} indicators, ensembles of cells within tissue can be effectively labelled in living animals for imaging. This bulk loading approach has been used successfully in diverse tissues in many species of animals (see diagram in Figure 1B). These include *C. elegans* (Jain *et al.*, 1993; Dal Santo *et al.*, 1999; Kerr *et al.*, 2000), *Drosophila* motor neurons (Karunanithi *et al.*, 1997) zebrafish nervous system (Gahtan *et al.*, 2002; Takahashi *et al.*, 2002), and mammalian brain (Ohki *et al.*, 2006; Takano *et al.*, 2007; Shummers *et al.*, 2008). In these experiments, cell-permeant AM ester forms of chemical dyes were microinjected into tissue *in vivo*. This results in labelling of a group of cells at the site of injection, which are then imaged using wide-field, confocal or two-photon microscopy techniques (Stosiek *et al.*, 2003; Takano *et al.*, 2007). Both the electroporation of cell impermeant indicators and bulk loading of cell permeant AM ester forms of Ca^{2+} indicators achieve universal labelling of all cell types in the vicinity of dye delivery. In the brain, this is a problem since both neurons and glial cells are simultaneously labelled. To overcome this problem a counterstaining approach has been used where specific cell types are stained *in situ* with a dye with different emission properties than the indicator. In bulk-loaded brain tissue, where both neurons and glial cells are labelled with indicator, sulfarhodamine 101 was used in conjunction to identify astrocytes. Astrocytes stained with sulfarhodamine 101 appear red, while OGB-1-AM, which fluoresces green monitors Ca^{2+} in both neurons and astrocytes (Nimmerjahn *et al.*, 2004; Shummers *et al.*, 2008).

Loading dye into specific neurons innervating a local area has also been achieved by two different means. In one, cell-permeant AM forms of chemical dyes were microinjected into axon tracks of known neural circuits which resulted in loading of the axons. Over time (4–24 h), the dye is transported in both anterograde and retrograde directions such that neuronal cell bodies and the nerve terminal regions were labelled, and these regions could be imaged without contamination of signal from non-neuronal cells (O'Donovan *et al.*, 1993; Kreitzer *et al.*, 2000). In another variation of this method, cell-impermeant, charged forms of dyes were microinjected into nerve fibre pathways such that some of the axons were damaged and the dye entered the cytoplasm which were then transported anterogradely to the cell bodies and imaged. Neural pathways in zebrafish spinal cord were injected with OGB-1 which resulted in specific labelling of neuronal cell bodies in the fish brain (Gahtan *et al.*, 2002). Similarly, Mauthner cell circuit in the zebrafish was labelled with calcium green dextran and imaged in the living fish (Takahashi *et al.*, 2002). These two specialized techniques for cell-specific dye loading are uniquely relevant only in the nervous system to image Ca^{2+} signals in collections of neurons with long processes, and may not be useful in other tissues.

Loading FPIs into cells

An alternative, newer technology for tissue and cell-specific indicator labelling is the development of genetically encodable, fluorescent, protein-based indicators (for reviews, see Knopfel *et al.*, 2006; Kotlikoff, 2007; Martin, 2008). The advantage of the

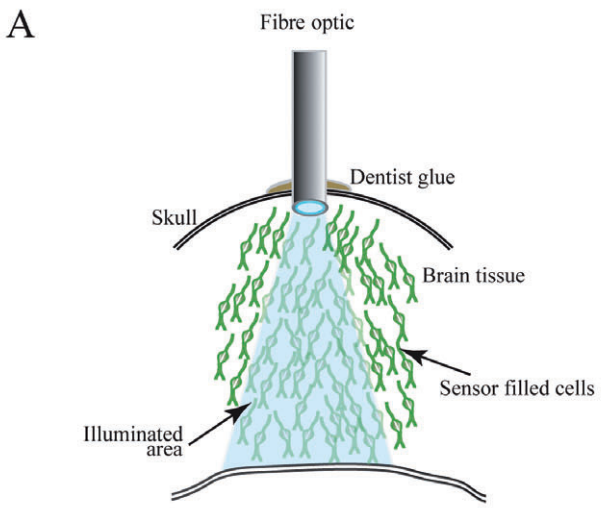
A
Fibre optic
Dentist glue
Skull
Brain tissue
Sensor filled cells
Illuminated area

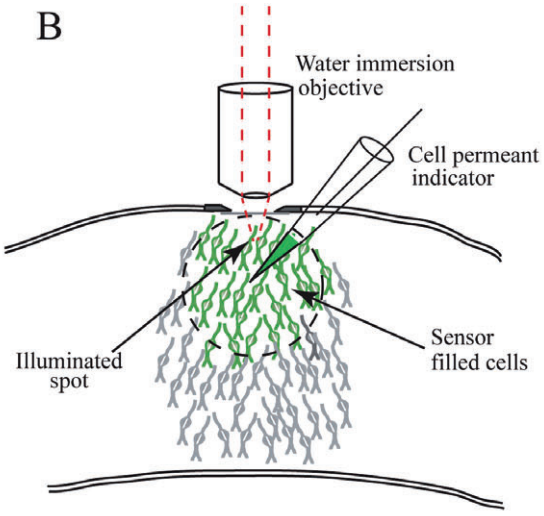
B
Water immersion objective
Cell permeant indicator
Illuminated spot
Sensor filled cells

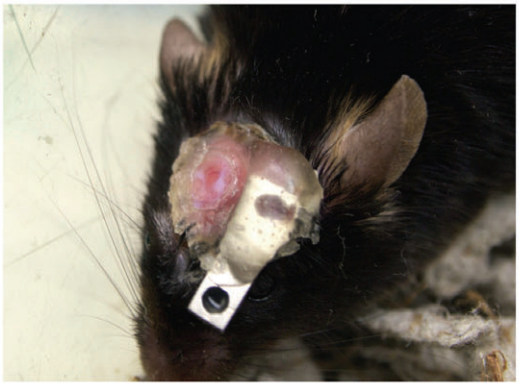
C


D

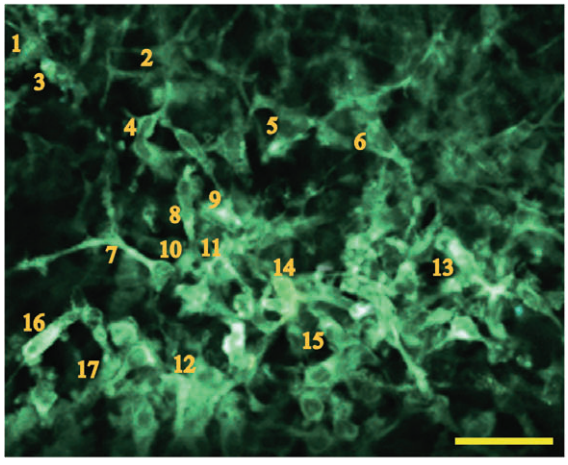
E
1
2
3
4
5
6
7
8
9
10
11
12
13
14
15
16
17

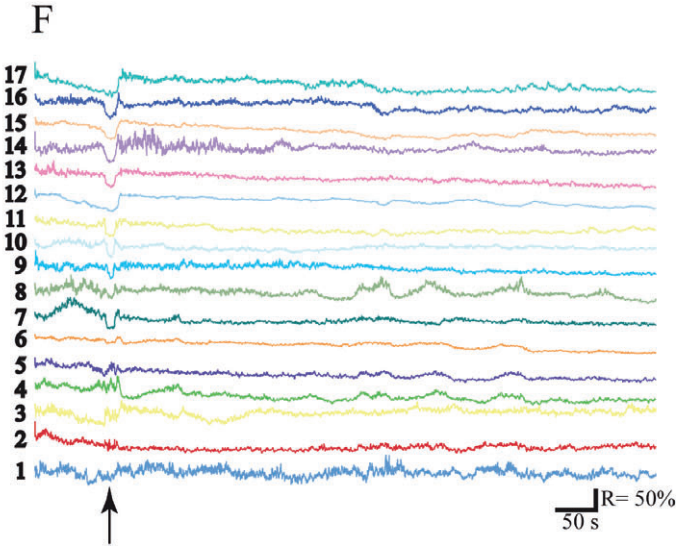
F
17
16
15
14
13
12
11
10
9
8
7
6
5
4
3
2
1
R= 50%
50 s

Figure 1

Different modes of transcranial imaging cortical cells using two-photon microscopy of a living mouse. A, Drawing of a fibre-optic endoscopic design for two-photon microscopy. The fibre is implanted and imaging is done in an awake, behaving mouse to image cortical neurons or glial cells. B, Imaging cortical cells through an acutely or chronically implanted cranial window. A glass coverslip is glued over a hole drilled through the skull using dental glue. In both cases, cells under the viewing port are labelled either by local injection of acetoxymethyl ester form of an organic dye or virus packaged fluorescent sensor, or transgenically expressed fluorescent Ca^{2+} sensor. C, Photograph of a mouse with an implanted cranial window. D, Photograph of transcranial two-photon imaging of an anaesthetized mouse with cranial window. These transgenic mice express the YC 3.60 cameleon in astrocytes under the control of the S-100b promoter. E, A field of astrocytes in the somatosensory cortex of the transgenic mouse imaged through the cranial window as in panel D. The image is an overlay of CFP and YFP channels. Images were acquired at 3 Hz. Scale = 50 μm. F, Spontaneous Ca^{2+} transients occurring in astrocytes numbered in panel E. Traces represent YFP/CFP ratios of intensities of pixels in regions of interest drawn around each cell, plotted against time. Data are from the author's laboratory.

genetically encoded Ca^{2+} indicators compared with synthetic dyes is the possibility of targeting the indicator specifically to the cells of interest, using plasmid designs containing specific promoters, and targeting sequences. Furthermore, this allowed for long-term imaging of Ca^{2+} signals discretely, not only in selected cell populations, but also in specific subcellular compartments in intact living animals. In addition, this allows for repeated imaging of the same tissue in the same animal. Both transfection techniques and transgenic technologies were readily available for long-term stable expression of indicators in the tissue of choice.

The most commonly used method to target FPIs to cells in animals is using transgenic methodologies (Heim *et al.*, 2007; Hendel *et al.*, 2008). Plasmids are engineered with FPI coding sequences with appropriate promoters to specifically target cells of interest in the model organism. Plasmids were then delivered to recipient cells using pronuclear injection, homologous recombination or retroviral transfer to early-stage embryos. Transgenic targeting of fluorescent proteins to specific cell types has been achieved to every organ in small invertebrates like *Drosophila* and large mammals, including primates. It is critical to choose particular promoters to avoid leaky expression to other cell types than the intended target. In addition, the level of expression of the fluorescent protein depends on how strong the promoter expression is. Ubiquitous expression of FPIs in all cells has also been carried out using promoters found in most cell types in the body such as β-actin (Nagai *et al.*, 2004). Specific expression of cameleons in neurons was achieved in transgenic mice using the promoters for the thy1 protein (Heim *et al.*, 2007). One caveat in using transgenic technology for cell-specific expression is that many promoters have strong context-sensitive expression patterns depending upon the site of transgene insertion. Therefore, expression patterns in different founder lines can differ widely. However, since large numbers of founders can be achieved, transgenic technology remains the method of choice for expression of fluorescent proteins in specific genetic lines.

DNA constructs containing appropriate promoters engineered with FPI coding sequences can also be packaged into plasmids and were transfected into cells using cell permeabilizing techniques such as liposome-mediated transfer or electroporation. Electroporation was used *in utero* to deliver plasmid constructs that direct expression of fluorescent proteins to embryonic brain (Petreanu *et al.*, 2009). Fluorescent proteins and FPIs have been directed to specific cells and cell groups both in brain and other tissues using viral vectors. In one experiment, YC 3.60 cameleon was packaged into an AAV (adenoassociated virus) vector to direct the FPI expression in neurons, which resulted in robust expression in various brain regions in mice. *In vivo* imaging of neural activity was successfully carried out in freely moving mice using a fibre-optic-based single-photon optical system (Wallace *et al.*, 2008; Lutcke *et al.*, 2010). In another study, pseudoherpes simplex virus vector was used to package another FPI, troponeon, and was delivered to cardiac muscle cells in a dog (Prorok *et al.*, 2009). Cell-specific expression using viral vectors are possible by using specific targeting strategies such as using Cre recombinase. A Cre-recombinase-dependent AAV was used to target a fluorescent protein in Cre-expressing transgenic mice to achieve specific labelling of cells in mouse brain (Petreanu *et al.*, 2009).

Synthetic organic dyes versus FPIs

One major advantage of using synthetic chemical indicators over FPIs is the wide range of indicators with widely differing Ca^{2+} affinities that are readily available commercially. It is also possible for the experimenter to introduce these dyes into cells with ease and use in experiments. Cell-loading conditions and protocols have been optimized over a number of years. Furthermore, in some instances, the synthetic organic Ca^{2+} indicators are superior to FPIs, in terms of the sensitivity, light throughput, signal-to-noise ratio, and dynamic range are considered. One particular disadvantage of organic synthetic dyes is they cannot be specifically targeted to particular

organelles or compartments in the cell. Although a number of strategies have been attempted to solve this problem, the results have been less than optimal (see Paredes *et al.*, 2008; Pozzan and Rudolf, 2009). In addition, they are at times compartmentalized into cellular organelles rendering them inaccessible in the cytoplasm (Del Nido *et al.*, 1998). To date, however, when signals deep within tissue need to be imaged with adequate signal-to-noise, at rates high enough to capture physiologically relevant events, synthetic dyes such as OGB-1 has been the indicators of choice (Grewe *et al.*, 2010).

Genetically encodable FPIs, however, are easily targeted to specific cell types in different organs in the body (Heim *et al.*, 2007), as well as to specific organelles such as endoplasmic reticulum or mitochondria (Pozzan and Rudolf, 2009). A major advantage of genetically encoded FPIs compared with synthetic dyes is the possibility of performing experiments over the long-term *in vivo* both at the single cell level and at subcellular levels (Kotlikoff, 2007). Furthermore, expressing FPIs within cells through genetic manipulations allows for repeated imaging of cells and circuits in the same animal over long periods of time. Thus both issues of development and functional plasticity can be studied. A number of different classes of chimeric designs of GFP and its mutated congeners have been engineered as useful Ca^{2+} indicators. Some of the new dyes such as G-CaMP3, TN-XXL and GA might turn out to be most useful tools for *in vivo* imaging. While much effort has yielded a number of fluorescent protein-based indicators, they still need further improvement. Currently available FPIs have narrow dynamic ranges compared with synthetic dyes, and in addition have slow response times. Though binding and unbinding time constants are not available for many of the FPIs, functional data suggest that under *in vivo* conditions, the kinetic properties of modern FPIs are not dramatically different from synthetic dyes like OGB-1. The decay time constant of Ca^{2+} transients in neuronal cell bodies measured *in vivo* using CerTN-L15 was 1.68 s (Heim *et al.*, 2007), which is only approximately twofold higher than the one measured with OGB-1 at 0.82 s (Kerr *et al.*, 2005). Indeed using d3cpv, a calmodulin and M13-based Ca^{2+} sensor expressed in mouse brain Ca^{2+} responses to single action potentials were reliably recorded as long as the firing rate did not exceed 1 Hz (Wallace *et al.*, 2008). The most recently developed G-CaMP3 appears to be well suited for imaging deep within brain tissue. This dye was recently utilized for imaging in motor cortex of mouse brain, and in a head-fixed fruit fly with good signal-to-noise ratios (Tian *et al.*, 2009; Seelig *et al.*, 2010). It would be important to make further improvements to increase the brightness, dynamic range and reduce response time constants of responses in FPIs such that physiological signals can be monitored in real time.

Imaging techniques

The earliest recordings of *in vivo* Ca^{2+} signals were made in preparations that were easily accessible for imaging. These were in invertebrates and small, transparent lower vertebrates and included *C. elegans* (Jain *et al.*, 1993), auditory system of the cricket (Sobel and Tank, 1994), olfactory system of the blowfly (Borst and Egelhaaf, 1992), honeybee (Galizia *et al.*, 1999) and zebrafish (Friedrich and Korsching, 1997). These early experiments on intact animals utilized organic synthetic Ca^{2+} indicator dyes and epifluorescence microscopy using CCD cameras. The use of zebrafish embryos was adopted early since they are small, transparent vertebrates and accessible to confocal microscopy when loaded with synthetic organic dyes (Ritter *et al.*, 2001). In combination with injection of indicator dyes and epifluorescence or confocal microscopies, various superficial structures, particularly sensory systems were investigated. The choice of these structures in invertebrate or small vertebrate animal models was mainly due to the extremely limited depth that could be imaged by conventional imaging techniques. Light scattering prevents recording fluorescence changes in cells using epifluorescence and confocal microscopy more than about 20 μm below the surface.

The advent of multiphoton laser scanning microscopy added a powerful tool for imaging cellular and subcellular structures even in highly scattering tissue. The concept of two-photon confocal microscopy was demonstrated by Denk *et al.* (1990), when they showed that fluorophores in living tissue can be excited with a stream of femtosecond infrared laser pulses. This principle was implemented in confocal microscopy and was quickly adopted by biologists for imaging isolated tissue and intact animals. This technology is undergoing continuous major technical developments. One important advantage of two-photon laser scanning microscopy is that it allows for imaging cells several hundred microns deep within tissue, enabling high-resolution functional imaging in living animals, including mammals. Innovative scanning technologies have been developed for ultrafast time-resolved imaging of large regions of tissue comprised of many cells in 3D space (Salome *et al.*, 2006; Duemani Reddy *et al.*, 2008; Grewe and Helmchen, 2009).

In vivo Ca^{2+} imaging using two-photon confocal microscopy is almost always implemented on a fixed-stage, upright microscope platform, which

requires the animal to be anaesthetized and immobilized with the imaged region exposed to the objective. Although motion due to respiration and pulse cannot be avoided, fixing the animal minimizes motion artefacts. Over the last decade a large number of functional Ca^{2+} imaging studies have been carried out using this approach in a number of organ systems and animal models (Svoboda *et al.*, 1999; Takano *et al.*, 2007; Mostany and Portera-Cailliau, 2008; Shummers *et al.*, 2008; see for review Helmchen and Kleinfeld, 2008). Most of this work focused on imaging activity in the brain, and a number of advances were realized. Imaging neuronal populations allows for simultaneous recordings of spontaneous and evoked responses in a large number of cells such that function of entire circuits can be inferred. By staining large populations of cells using strategies of injecting a bolus of cell permeant form of organic dyes (Garaschuk *et al.*, 2006), injection of dextran conjugated dye into axon bundles (Hirase *et al.*, 2004), or using viral infection using FPI packaged into viral vectors (Mank *et al.*, 2008), large populations of neurons can be imaged using these methods for simultaneous recordings of spontaneous activity (Adelsberger *et al.*, 2005) as well as evoked responses (Tabor *et al.*, 2004). Various brain regions such as the olfactory bulb (Wachowiak *et al.*, 2004), cerebellum (Diez-Garcia *et al.*, 2007), visual cortex (Ohki *et al.*, 2006) and somatosensory cortex (Stosiek *et al.*, 2003) have been imaged. In the brain, the bulk loading of cells followed by two-photon microscopy allowed for single cell resolution and revealed the precisely ordered pinwheel centres in the visual cortex of cats (Ohki *et al.*, 2006). Recent experiments in mice using particularly organic Ca^{2+} indicators such as OGB-1, and ultrafast imaging techniques neural network activity was recorded in collections of cells at rates exceeding 0.5 kHz (Grewe *et al.*, 2010; Lutcke *et al.*, 2010). Ca^{2+} transients in response to single action potentials were recorded with signal-to-noise ratios in the order of 2–5 enabling determination of spike times with millisecond precision.

Because the zebrafish embryos are transparent, they were most suitable for developmental studies. Two-photon imaging of larvae revealed that retinal ganglion cell axonal arbors in the optic tectum develops rapidly and this development depends upon activity-dependent competition between neighbouring axons (Hua *et al.*, 2005). A separate two-photon imaging study of tectal neurons showed that soon after dendritic outgrowth and synaptogenesis, most visual properties were already fully established. This development did not require complex visual experience (Niell and Smith, 2005). This type or *in vivo* two-photon Ca^{2+} imaging in the visual cortex and olfactory bulb of zebrafish embryos were most useful in establishing the functional topology of neuronal activity patterns, and also allowed for analysis of the role of activity in circuit development (Wachowiak *et al.*, 2004; Yaksi *et al.*, 2007).

One major problem with bolus loading of large populations of cells is that all the different types of cells such as neurons and glial cells in the region are labelled. Different strategies are available to solve this problem at least partially. As mentioned earlier, sulfarhodamine 101 was successfully used to identify astrocytes during imaging experiments (Nimmerjahn *et al.*, 2004; Winship *et al.*, 2007). Another method is labelling by microinjection of axonal bundles with dextran conjugated indicators and using axonal transport over several hours to both retrogradely and anterogradely label neurons prior to imaging (Hirase *et al.*, 2004). This approach has been successfully used in the olfactory bulb (Oka *et al.*, 2006) and in the cerebellar olivary nucleus (Kreitzer *et al.*, 2000). This approach of retrograde labelling the olfactory system in the *Drosophila* revealed that odorant receptor-specific glomeruli showed different ligand spectra and much higher sensitivity *in vivo* compared with similar experiments *in vitro* (Oka *et al.*, 2006). The problem of specific labelling is also effectively solved by the use of genetically encodable FPIs to target cells by the use of cell-specific promoters (Knopfel *et al.*, 2006; Mank *et al.*, 2008; Atkin *et al.*, 2009). Figure 1E,F shows an example of two-photon imaging of astrocytes in the somatosensory cortex specifically expressing YC 3.60 sensor in a transgenic mouse (see also Atkin *et al.*, 2009). This approach was successfully used to study parallel fibre pathway activation in the cerebellum in mice expressing G-CaMP2 in neurons *in vivo* (Diez-Garcia *et al.*, 2007). These authors succeeded in measuring Ca^{2+} transients in beams of parallel fibres through the intact skull. In another study, the cameleon YC 3.1 was expressed in *Drosophila* flight muscles to record Ca^{2+} transients in the myoplasm while simultaneously recording the power output of the muscle (Gordon and Dickinson, 2006). Similarly G-CaMP2 was expressed in the cardiac muscles in transgenic mice to record Ca^{2+} transients associated with the heartbeat in developing hearts within embryos (Tallini *et al.*, 2006). The authors were able to describe the organization of atrioventricular conduction and the development of the atrioventricular node. In the brain, the non-invasive nature of *in vivo* Ca^{2+} imaging research alters the research focus to recording from central nervous system microcircuits, opening the door for systems neuroscience. Furthermore, technical innovations yielded methods for routine transcranial imaging

(Helmchen and Kleinfeld, 2008; Mostany and Portera-Cailliau, 2008), including repeated imaging of the same neural circuits in a given individual animal over a period of weeks and months (Holtmaat *et al.*, 2006; Mostany and Portera-Cailliau, 2008). Cortical circuits were imaged in a head-fixed position through a transparent cranial window, implanted under anaesthesia. These methods proved to be a boon to the burgeoning research in the neurosciences over the last decade allowing investigation of communication within neural microcircuits in the brain.

More recently, efforts have been underway to develop techniques to image tissue with cellular level resolution in awake, behaving animals. In one method, transcranial imaging of cellular Ca^{2+} signals was carried out in an anaesthetized, head-fixed mouse to study signalling in the cortical layers (Dombeck *et al.*, 2007). Ca^{2+} signals were recorded in layer 2/3 cortical pyramidal neurons and astrocytes loaded with calcium green-1 in response to sensory stimuli. Technological innovations are sorely needed to improve imaging in unanaesthetized, freely moving animals. Several technical hurdles need to be overcome to realize this goal. First, the microscopes must be sufficiently small to be borne by the animal which is freely mobile. Second, the device should retain the functionality of the conventional microscope. Thirdly, the instrument must be robust enough to minimize voluntary and involuntary tissue motion artefacts. Realizing all three of these goals has been difficult, but work towards them took a decisive step forward with the invention of a fibre-optic-based miniature two-photon microendoscope which could be mounted on a rat or a mouse (see Figure 1A for diagram) (Helmchen *et al.*, 2001). This device incorporated fibre optics to bring in both the excitation beam and to collect the emitted light from cortical pyramidal neurons in awake animals (Helmchen *et al.*, 2001). Although this form of imaging suffers from restricted field of view and low spatial resolution, it offers excellent temporal resolution, and can report from large cellular ensembles (Grewe and Helmchen, 2009; Grewe *et al.*, 2010). In the brain, microendoscopic, two-photon microscopy affords monitoring synchronous activity within entire neural circuits, and can be used to study any region of the brain (Adelsberger *et al.*, 2005). The microendoscopes use a novel approach involving the use of micro-electro-mechanical scanners coupled with gradient-index (GRIN) lenses on optical fibres has been developed (Gobel *et al.*, 2004; Engelbrecht *et al.*, 2008; Murayama and Larkum, 2009). These engineering developments made miniaturizing the scanning device possible while allowing for a fibre-optic tether. Since the GRIN lens refracts light through a refractive index gradient, its optical surfaces are flat and allows for efficiently focusing and collecting light, while keeping the overall form factor small. While much work is focused on recording Ca^{2+} signals in neural circuits in the brain, microendoscopy in non-neural tissue has remained in the sphere of diagnostic endoscopy, and is routine in the diagnosis of gastrointestinal and airway pathologies (see Tsesmeli and Coumaros, 2009 for review). Thus far, fibre-optic-based microendoscopy systems have not achieved comparable optical image quality to that of stage-mounted, fixed microscopes in recording cellular Ca^{2+} signals in tissue. Technical innovation to improve fibre-optic, microendoscopic, two-photon microscopy is necessary since imaging awake, freely behaving animals is ultimately required to address many physiological questions in *in vivo* studies.

Recently, in a technical *tour de force*, scientists have developed methods to train mice to cooperate in imaging experiments using two-photon microscopy (Sato and Svoboda, 2010). Svoboda and colleagues have carried out transcranial imaging in head-fixed, awake behaving mice and succeeded in recording Ca^{2+} signals from neural circuits in the barrel cortex associated with sensory-motor activity (Komiyama *et al.*, 2010; O'Connor *et al.*, 2010). In one study, the functional properties of barrel cortex neurons projecting to the primary motor cortex was imaged. The authors found that neurons projecting to the primary motor cortex have large receptive fields showing that intermingled neurons in the primary sensory areas send specific stimulus features to different parts of the brain (Sato and Svoboda, 2010). In another series of experiments, mice were trained to respond with a specific behaviour, that is, lick for a water reward, in response to particular odours and not produce the behaviour (not lick) for another odour. Cortical neurons were imaged during this behaviour through a cranial window, and the authors were able to identify two non-overlapping tongue motor cortex areas (Komiyama *et al.*, 2010). Many neurons in these regions showed modulation coinciding with or preceding the licking action, consistent with their involvement in motor control. Furthermore, they found that nearby neurons showed profound coincident activity and that this temporal correlation in activity increased as task learning progressed, suggesting a learning related structural plasticity (Komiyama *et al.*, 2010). The same group of researchers, in another set of experiments, trained mice to respond to a whisking cue with a specific behaviour (lick water) and not lick if the whisking cue was out of reach of the whiskers (O'Connor *et al.*, 2010). Mice had to learn

to lick if the pole was in the go position (within reach of the whiskers) and not lick when the pole was in the no-go position (out of reach of whiskers). Cortical circuit activity was recorded as sensory neuronal Ca^{2+} signals to map the local circuit that regulates sensory-motor function. Mice learnt this complex task in 1–2 weeks and performed localizations using a sophisticated strategy that is expected to yield large differences in barrel cortex activity patterns for the different trial types. Mice maximized whisker contact with the go stimulus and minimized contact with the no-go stimulus. It is likely that this motor strategy produces very different patterns of activity across the barrel cortex for go and no-go trials, and this might help the mouse choose between go and no-go responses (O'Connor *et al.*, 2010).

In a parallel development, innovations in the use of chimeric aequorin-GFP (GA) constructs have been advanced by a group of researchers for *in vivo* Ca^{2+} imaging in awake freely moving animals (Curie *et al.*, 2007); (see for review Martin *et al.*, 2007). The luminescent biosensor is genetically encoded into the tissue of interest, and the animals are imaged using high sensitivity electron-multiplying CCD cameras (Rogers *et al.*, 2008; Roncali *et al.*, 2008). Awake, behaving animals are imaged over long periods of time albeit with relatively poor spatial resolution. While this method affords reasonable temporal resolution, cellular resolution in space is rarely possible, which is a major disadvantage. The signal-to-noise, however, is excellent due to the total absence of autofluorescence, since no optical excitation is necessary. Ca^{2+}-induced aequorin luminescence is amplified by resonance energy transfer to GFP (Shimomura *et al.*, 1993; Curie *et al.*, 2007). This approach will have to await the invention of super-sensitive image capture devices to realize the spatial and temporal resolution necessary to make it a useful tool for *in vivo* Ca^{2+} imaging.

Ca^{2+} imaging in disease states

Ca^{2+} imaging has been used to study various disease states for some time using animal models in *in vitro* studies, mostly in cell culture ad brain slice preparations. Recently, however, novel imaging methods with cellular resolution have been used more and more for investigation of disease models *in vivo* with the goal of a detailed characterization of the pathophysiology. Since many disease states are not faithfully reproduced in *in vitro* models, this development holds much promise. Furthermore, the problems in depth penetration during imaging prevents access to deeper regions of the brain and other tissues. However, the availability of genetic tools significantly adds to development of *in vivo* imaging techniques to investigate disease states. A wide variety of transgenic mice are now available, which are models of neurological disease, and mice with specific cell types or cellular compartments labelled with indicators have become valuable tools.

Two-photon Ca^{2+} imaging has been used in the study of glial cells signalling in the brain (Hirase *et al.*, 2004; Atkin *et al.*, 2009). Recent *in vivo* studies showed that astrocytes show rapid Ca^{2+} transients upon sensory stimulation, and these signals are perfectly tuned to the neuronal signals in the vicinity (Wang *et al.*, 2006; Shummers *et al.*, 2008). Astrocytes also have a role in regulation of local blood flow by regulating blood vessel diameter (Takano *et al.*, 2006). Astrocytes are involved in many normal and pathological brain functions and may represent a promising therapeutic target. Astrocytes have been implicated in epilepsy, stroke and Alzheimer's disease (Tian *et al.*, 2005; Takano *et al.*, 2007). A recent *in vivo* study of an Alzheimer's disease mouse model revealed a number of new observations including rapid development local neuronal toxicity, appearance of dysmorphic neurites and microglial infiltration (Meyer-Luehmann *et al.*, 2008). In a mouse model of Alzheimer's disease, astrocytic Ca^{2+} homeostasis and Ca^{2+} signals were recorded *in vivo* using OGB-1 as the indicator (Kuchibhotla *et al.*, 2009). Synchronously coordinated, rapidly spreading Ca^{2+} waves were recorded in these animals (Kuchibhotla *et al.*, 2009). The Ca^{2+} waves originated near Alzheimer's plaques and radially spread over hundreds of micrometers. A recent review summarizes much of the imaging data on Alzheimer models available to date (Dong *et al.*, 2010).

Progressive axonal and neuromuscular junction alterations in mice with different gene mutations were identified by fibre-optic-based confocal microendoscopy *in vivo* (Wong *et al.*, 2009). This group were able to visualize YFP expression in peripheral nerves and follow motor neuronal degeneration in *Wld^s* (Wollerian degeneration spontaneous mutant) mice. In addition, the modification of motor neuron degeneration in *Wld^s* mice by mutating N-ethyl-n-nitrosourea was characterized. Furthermore, in the same study, motor neuron degeneration in Sod1 mutation was also followed by confocal imaging (Wong *et al.*, 2009). Two-photon confocal microscopy was applied to visualize changes in microvasculature in the brain more than a decade ago (Kleinfeld *et al.*, 1998). Using this approach the development of stroke and its pathophysiology have been studied using two-photon microscopy. These studies have revealed the rapid changes to dendritic spine structure during ischaemia (Zhang and Murphy, 2007). The extent of the functional

recovery upon restoration of normal blood flow after ischaemia was also characterized. Furthermore, this approach allowed for rapidly alternating between ischaemia and reperfusion while monitoring functional alterations in the brain. This study revealed that the apical dendritic structure in layer V cortical neurons was dramatically degraded by ischaemia (Murphy *et al.*, 2008).

Epilepsy is another common neurological disorder that has been investigated using *in vivo* Ca^{2+} imaging. Epilepsy is characterized by recurrent seizure activity caused by bursts of synchronous and rhythmic neural circuit hyperactivity. Intrinsic optical signals were monitored in the very first *in vivo* studies of epileptic seizures (Schwartz and Bonhoeffer, 2001).Two-photon imaging was used in brain slice preparations in models of epileptic seizures to achieve single cell resolution (Badea *et al.*, 2001). *In vivo* Ca^{2+} imaging was first used for investigation of astrocytic activity during seizure events (Tian *et al.*, 2005). Two-photon Ca^{2+} imaging *in vivo* showed that astrocytic Ca^{2+} signals were strongly correlated with the epileptogenic neuronal bursting activity in this animal model (Tian *et al.*, 2005). In a recent study, an *in vivo* seizure model was developed in an albino *Xenopus laevis* tadpole where pentylenetetrazol-induced seizure activity was directly monitored (Hewapathirane *et al.*, 2008). *In vivo* Ca^{2+} imaging is being increasingly used to investigate a number of neurological diseases in animal models. It is quite likely that similar experimental approaches would be valuable in other organ systems as well. Two-photon microendoscopy designs could become potentially valuable tools to investigate the pathophysiology and disease progression in other metabolic and endocrine disorders.

While *in vivo* Ca^{2+} imaging has become a centrepiece of research in physiological and cell biological processes, it is only rarely used as a tool in pharmacological research. High-throughput Ca^{2+} imaging is increasingly utilized in multi-well sample configurations in drug discovery research, particularly for screening of unknown compounds (Miret *et al.*, 2005). *In vivo* Ca^{2+} imaging could potentially play an important role in pharmacological characterization of potential drugs. It might be possible to record drug effects on cellular Ca^{2+} signals *in vivo* in transgenic animals expressing fluorescent Ca^{2+} indicators in specific tissues. For example, animals expressing genetically encodable Ca^{2+} indicators in neurons or astrocytes can be imaged to monitor actions of a given drug on activity in specific networks in accessible regions of the cortex. Similarly, *in vivo* imaging of different splanchnic organs with a multiphoton microscope or a fibre-optic-based microendoscope may be possible to monitor drug effect on the liver, pancreas and kidney. The newly developed luminescence-based indicators such as GA would also be useful to image internal organs in real time albeit in somewhat lower resolution than with fluorescence imaging. However, very little published work exists on this line of work in the literature until now.

Technical considerations

As discussed earlier, there are a number of options available for filling cells with Ca^{2+} indicators for *in vivo* Ca^{2+} imaging. Of these, filling single cells by microinjection provides the most discrete, high signal-to-noise, high contrast fluorescence signals (Sobel and Tank, 1994; Helmchen *et al.*, 1999). However, since most *in vivo* imaging applications target cell–cell communication and signalling within cellular ensembles, it is often necessary to fill populations of cells in local areas within tissue. In the brain, most investigations target local microcircuits that contain in the order of 1000–10 000 cells which are synaptically connected. This is achieved by various means, and the most often used is multicell bulk loading with either cell permeant synthetic organic dyes (Stosiek *et al.*, 2003; Shummers *et al.*, 2008), passive diffusion techniques (Zimprich *et al.*, 1998; Takahashi *et al.*, 2002) or local electroporation (Nagayama *et al.*, 2007). Genetically encodable, fluorescent, protein-based indicators are expressed in cells using local application of plasmids followed by electroporation (Tabata and Nakajima, 2001; Mank *et al.*, 2008; Holtmaat *et al.*, 2009), or using plasmids packaged in viral vectors (Dittgen *et al.*, 2004; Mank *et al.*, 2008; Holtmaat *et al.*, 2009). In all of these methods, cell populations are filled with indicators. The most selective labelling is generally achieved through transgenic technologies using any one of the genetically encodable Ca^{2+} sensors engineered to be expressed under the control of cell-specific promoters (see Mank *et al.*, 2008).

Imaging *in vivo* with cellular resolution requires data sampling from many hundreds of cells with good temporal resolution, and this is not trivial. In normal scanning mode, the laser is scanned within one focal plane in a raster-like fashion. Using this approach, data acquisition is slow, since the scan pattern needs to be repeated several times to image large fields. A number of alternative strategies have been developed to achieve more flexibility in imaging large areas in three dimensions. Entirely new scanning regimes need to be developed to increase speed of data collection and to acquire images in 3D space, since local neural circuits in the brain are distributed in 3D volume of brain tissue (Grewe and Helmchen, 2009; Grewe *et al.*, 2010). In order to image physiological signals in such circuits

with good temporal resolution, novel high-speed xy scan techniques were developed (Gobel and Helmchen, 2007; Grewe *et al.*, 2010; Lutcke *et al.*, 2010). A recent review elegantly addresses many of the imaging techniques and the technical innovations that were developed to realize them (Gobel and Helmchen, 2007; Tian *et al.*, 2009; Grewe *et al.*, 2010). Innovations using resonant scanners such as acousto-optical devices (AODs) for random access scanning in 2D, and the use of multiple AODs, provided inertia-free, fast scanning in 3D (Hammond and Glick, 2000; Nguyen *et al.*, 2001; Gobel and Helmchen, 2007; Grewe *et al.*, 2010). With fibre optic illumination to predestined locations by positioning fibre tips appropriately, 3D measurements of in the order of 1000 cells with 100-Hz temporal resolution was achieved (Rozsa *et al.*, 2007; Lutcke *et al.*, 2010). These technological innovations have greatly extended the utility of two-photon laser scanning microscopy for *in vivo* imaging.

Steady technical innovations over the last decade have provided the tools necessary for imaging Ca^{2+} signals in the living animal with near real-time temporal resolution in 3D space deep within tissue. In conjunction with multi-cell bolus loading and two-photon laser scanning microscopy, large neuronal populations in the brain have been imaged with cellular resolution (Winship *et al.*, 2007; Shummers *et al.*, 2008; Grewe *et al.*, 2010; Lutcke *et al.*, 2010). The capability to image large scale structures revealed the extraordinary variability of odorant receptor maps in the olfactory bulb in mice and led to the finding that the receptor-defined olfactory glomeruli *in vivo* showed very high sensitivities compared with pericams in *in vitro* experiments (Oka *et al.*, 2006). The availability of methods for *in vivo* Ca^{2+} imaging provided the means for directly imaging astrocytes as they monitor neuronal activity in a functioning neural network in the brain, providing the first direct experimental evidence for neuronal-glial cell signalling (Winship *et al.*, 2007; Shummers *et al.*, 2008). Imaging specific cell types in tissues was achieved with the different genetically encodable indicators such as G-CaMP2, G-CaMP3 and TN-XXL which can be targeted to defined populations of cells using specific promoters in transgenic animals (Hendel *et al.*, 2008; Lutcke *et al.*, 2010). This allows for discretely recording activity within defined cellular networks in the brain such as recording parallel fibre-Purkinje cell synapses in the living animal. Ca^{2+} signals in astrocytic networks in response to neural activity for sensory stimulation (forepaw stimulation) was imaged in transgenic mice expressing the YC 3.60 cameleon in astrocytes (Atkin *et al.*, 2009). While these genetically encoded probes initially did not perform as well in mice compared with *C. elegans* or zebrafish, the new constructs are superior and have been shown to detect Ca^{2+} signals in response to single action potentials and responses to very low network firing rates (Tian *et al.*, 2009; Lutcke *et al.* 2010). In the brain, detection of Ca^{2+} signals from dendrites and dendritic spines is extremely difficult because of very low indicator content within them. Image contrast is also poor, since in addition to cells, the many fine processes in the surrounding neuropil are also stained. Single cell microinjection was the only technique that provided sufficient contrast in isolated tissue slice preparations, which is not easily done in living animals. This problem may now be partially solved with the use of novel indicators and ultrafast 3D volume imaging in two-photon laser scanning microscopy (Gobel and Helmchen, 2007; Tian *et al.*, 2009; Grewe *et al.*, 2010; Lutcke *et al.*, 2010). In this respect organic indicators are superior for high-speed imaging of Ca^{2+} transients in response to action potential trains. OGB-1 has been successfully used in a number of recent studies to record activity in neuronal microcircuits at rates better than 200 Hz (Grewe *et al.*, 2010). *In vivo* optical imaging of brain function has benefited most from the developments in two-photon laser scanning microscopy, and similar advances in imaging Ca^{2+} signals *in vivo* are eagerly anticipated in other organ systems.

Future outlook

Most of the effort in imaging cellular Ca^{2+} signals *in vivo* has been focused on the nervous system. Now that the instrumentation and methods have been developed for brain imaging, they can be applied to other organ systems in the near future. *In vivo* Ca^{2+} imaging potentially could be used to monitor altered signalling in disease states including cancer, and such detection systems could provide a platform for pharmacological testing and drug development. In the brain, *in vivo* Ca^{2+} imaging is proving to be an invaluable tool to investigate disease states that were not accessible to *in vitro* experimentation, because isolated brain slices from diseased and aged brain are of poor quality. In the nervous system, combining Ca^{2+} imaging with electrophysiology and behavioural approaches is poised to yield important data for understanding the neural code for complex behaviours including learning and memory. Further advances in cellular labelling and imaging techniques, especially ultrafast 3D imaging tools, are imminent and expected to enable imaging of large populations of cells in the brain. Improvements in

indicators, including genetically encoded indicators, will facilitate functional characterization of microcircuits in the brain and animal models of neurological disorders. Although two-photon laser scanning microscopy provides better depth penetration compared with wide-field microscopy, *in vivo* two-photon imaging is still restricted to very superficial layers of a mouse brain. Improved technologies would be necessary for imaging in deeper layers of the brain and indeed other tissues. Improvements in indicators and image sensors would be required to achieve this goal. Bioluminescence-based probes such as GA could become useful for cellular level imaging deep within tissue if appropriate light transmission technologies and super-sensitive sensors with large pixel formats become available. Optimization of fluorescence signal detection and improved signal analysis tools are expected and should provide methods for single spike detection in 3D neural networks. Improved brightness and signal-to-noise in indicators should help to accelerate development of methods to image tissue in awake, freely moving animals. In this regard, the optimization of microendoscopic design and miniaturization should spur *in vivo* imaging in all organ systems, particularly the brain. The availability of microendoscopes should make *in vivo* imaging generally possible for all organ systems since *trans*-integumental imaging using endoscopes are already in routine diagnostic use. *In vivo* imaging using microendoscopic, two-photon microscopy would be expected to provide experimental models for testing effectiveness of drugs in specific disease states such as epilepsy, cancer, animal models of diseases of the liver and pancreas. Finally, *in vivo* imaging of animals trained for imaging without anaesthesia while engaged in complex behaviours is expected to yield important data on physiological communication within cellular networks in different organ systems.

Acknowledgements

Many thanks to Ms Lynne Holtzclaw, Dr Alessandro Fatatis and Dr Andra E. Miller for critical reading of the manuscript and painstaking proofing and editing.

Conflict of interest

I can categorically certify that there are no conflicts to declare.

References

Adelsberger H, Garaschuk O, Konnerth A (2005). Cortical calcium waves in resting newborn mice. Nat Neurosci 8: 988–990.

Atkin SD, Patel S, Kocharyan A, Holtzclaw LA, Weerth SH, Schram V *et al*. (2009). Transgenic mice expressing a cameleon fluorescent Ca2+ indicator in astrocytes and Schwann cells allow study of glial cell Ca2+ signals *in situ* and *in vivo*. J Neurosci Methods 181: 212–226.

Badea T, Goldberg J, Mao B, Yuste R (2001). Calcium imaging of epileptiform events with single-cell resolution. J Neurobiol 48: 215–227.

Baird GS, Zacharias DA, Tsien RY (1999). Circular permutation and receptor insertion within green fluorescent proteins. Proc Natl Acad Sci U S A 96: 11241–11246.

Baker PF, Hodgkin AL, Ridgway EB (1971). Depolarization and calcium entry in squid giant axons. J Physiol 218: 709–755.

Baubet V, Le Mouellic H, Campbell AK, Lucas-Meunier E, Fossier P, Brulet P (2000). Chimeric green fluorescent protein-aequorin as bioluminescent Ca2+ reporters at the single-cell level. Proc Natl Acad Sci U S A 97: 7260–7265.

Bootman MD, Berridge MJ (1995). The elemental principles of calcium signaling. Cell 83: 675–678.

Borst A, Egelhaaf M (1992). *In vivo* imaging of calcium accumulation in fly interneurons as elicited by visual motion stimulation. Proc Natl Acad Sci U S A 89: 4139–4143.

Chaigneau E, Tiret P, Lecoq J, Ducros M, Knopfel T, Charpak S (2007). The relationship between blood flow and neuronal activity in the rodent olfactory bulb. J Neurosci 27: 6452–6460.

Cheung CY, Webb SE, Meng A, Miller AL (2006). Transient expression of apoaequorin in zebrafish embryos: extending the ability to image calcium transients during later stages of development. Int J Dev Biol 50: 561–569.

Creton R, Steele ME, Jaffe LF (1997). Expression of apo-aequorin during embryonic development; how much is needed for calcium imaging? Cell Calcium 22: 439–446.

Cubitt AB, Heim R, Adams SR, Boyd AE, Gross LA, Tsien RY (1995). Understanding, improving and using green fluorescent proteins. Trends Biochem Sci 20: 448–455.

Curie T, Rogers KL, Colasante C, Brulet P (2007). Red-shifted aequorin-based bioluminescent reporters for *in vivo* imaging of Ca2 signaling. Mol Imaging 6: 30–42.

Dal Santo P, Logan MA, Chisholm AD, Jorgensen EM (1999). The inositol trisphosphate receptor regulates a 50-second behavioral rhythm in *C. elegans*. Cell 98: 757–767.

Dani JW, Chernjavsky A, Smith SJ (1992). Neuronal activity triggers calcium waves in hippocampal astrocyte networks. Neuron 8 (Pt 1): 429–440.

Del Nido PJ, Glynn P, Buenaventura P, Salama G, Koretsky AP (1998). Fluorescence measurement of calcium transients in perfused rabbit heart using rhod 2. Am J Physiol 274 (Pt 2): H728–H741.

Denk W, Strickler JH, Webb WW (1990). Two-photon laser scanning fluorescence microscopy. Science 248: 73–76.

Diez-Garcia J, Akemann W, Knopfel T (2007). *In vivo* calcium imaging from genetically specified target cells in mouse cerebellum. Neuroimage 34: 859–869.

Dipolo R, Requena J, Brinley FJ Jr, Mullins LJ, Scarpa A, Tiffert T (1976). Ionized calcium concentrations in squid axons. J Gen Physiol 67: 433–467.

Dittgen T, Nimmerjahn A, Komai S, Licznerski P, Waters J, Margrie TW *et al.* (2004). Lentivirus-based genetic manipulations of cortical neurons and their optical and electrophysiological monitoring *in vivo*. Proc Natl Acad Sci U S A 101: 18206–18211.

Dombeck DA, Khabbaz AN, Collman F, Adelman TL, Tank DW (2007). Imaging large-scale neural activity with cellular resolution in awake, mobile mice. Neuron 56: 43–57.

Dong J, Revilla-Sanchez R, Moss S, Haydon PG (2010). Multiphoton *in vivo* imaging of amyloid in animal models of Alzheimer's disease. Neuropharmacology 59: 268–275.

Drobac E, Tricoire L, Chaffotte AF, Guiot E, Lambolez B (2010). Calcium imaging in single neurons from brain slices using bioluminescent reporters. J Neurosci Res 88: 695–711.

Duemani Reddy G, Kelleher K, Fink R, Saggau P (2008). Three-dimensional random access multiphoton microscopy for functional imaging of neuronal activity. Nat Neurosci 11: 713–720.

Duffy S, MacVicar BA (1995). Adrenergic calcium signaling in astrocyte networks within the hippocampal slice. J Neurosci 15: 5535–5550.

Engelbrecht CJ, Johnston RS, Seibel EJ, Helmchen F (2008). Ultra-compact fiber-optic two-photon microscope for functional fluorescence imaging *in vivo*. Opt Express 16: 5556–5564.

Friedrich RW, Korsching SI (1997). Combinatorial and chemotopic odorant coding in the zebrafish olfactory bulb visualized by optical imaging. Neuron 18: 737–752.

Gahtan E, Sankrithi N, Campos JB, O'Malley DM (2002). Evidence for a widespread brain stem escape network in larval zebrafish. J Neurophysiol 87: 608–614.

Gahwiler BH (1981). Organotypic monolayer cultures of nervous tissue. J Neurosci Methods 4: 329–342.

Galizia CG, Sachse S, Rappert A, Menzel R (1999). The glomerular code for odor representation is species specific in the honeybee Apis mellifera. Nat Neurosci 2: 473–478.

Garaschuk O, Milos RI, Konnerth A (2006). Targeted bulk-loading of fluorescent indicators for two-photon brain imaging *in vivo*. Nat Protoc 1: 380–386.

Garaschuk O, Griesbeck O, Konnerth A (2007). Troponin C-based biosensors: a new family of genetically encoded indicators for *in vivo* calcium imaging in the nervous system. Cell Calcium 42: 351–361.

Gaspers LD, Thomas AP (2005). Calcium signaling in liver. Cell Calcium 38: 329–342.

Gobel W, Helmchen F (2007). *In vivo* calcium imaging of neural network function. Physiology (Bethesda) 22: 358–365.

Gobel W, Kerr JN, Nimmerjahn A, Helmchen F (2004). Miniaturized two-photon microscope based on a flexible coherent fiber bundle and a gradient-index lens objective. Opt Lett 29: 2521–2523.

Gordon S, Dickinson MH (2006). Role of calcium in the regulation of mechanical power in insect flight. Proc Natl Acad Sci U S A 103: 4311–4315.

Grewe BF, Helmchen F (2009). Optical probing of neuronal ensemble activity. Curr Opin Neurobiol 19: 520–529.

Grewe BF, Langer D, Kasper H, Kampa BM, Helmchen F (2010). High-speed *in vivo* calcium imaging reveals neuronal network activity with near-millisecond precision. Nat Methods 7: 399–405.

Griesbeck O, Baird GS, Campbell RE, Zacharias DA, Tsien RY (2001). Reducing the environmental sensitivity of yellow fluorescent protein. Mechanism and applications. J Biol Chem 276: 29188–29194.

Grynkiewicz G, Poenie M, Tsien RY (1985). A new generation of Ca2+ indicators with greatly improved fluorescence properties. J Biol Chem 260: 3440–3450.

Guerrero G, Reiff DF, Agarwal G, Ball RW, Borst A, Goodman CS *et al.* (2005). Heterogeneity in synaptic transmission along a *Drosophila* larval motor axon. Nat Neurosci 8: 1188–1196.

Hammond AT, Glick BS (2000). Raising the speed limits for 4D fluorescence microscopy. Traffic 1: 935–940.

Hasan MT, Friedrich RW, Euler T, Larkum ME, Giese G, Both M *et al.* (2004). Functional fluorescent Ca2+ indicator proteins in transgenic mice under TET control. PLoS Biol 2: e163.

Hastings JW, Mitchell G, Mattingly PH, Blinks JR, Van Leeuwen M (1969). Response of aequorin bioluminescence to rapid changes in calcium concentration. Nature 222: 1047–1050.

He J, Ma L, Kim S, Nakai J, Yu CR (2008). Encoding gender and individual information in the mouse vomeronasal organ. Science 320: 535–538.

Heim R, Prasher DC, Tsien RY (1994). Wavelength mutations and posttranslational autoxidation of green fluorescent protein. Proc Natl Acad Sci U S A 91: 12501–12504.

Heim N, Garaschuk O, Friedrich MW, Mank M, Milos RI, Kovalchuk Y *et al.* (2007). Improved calcium imaging in transgenic mice expressing a troponin C-based biosensor. Nat Methods 4: 127–129.

Helmchen F, Kleinfeld D (2008). Chapter 10. *In vivo* measurements of blood flow and glial cell function with two-photon laser-scanning microscopy. Methods Enzymol 444: 231–254.

Helmchen F, Svoboda K, Denk W, Tank DW (1999). *In vivo* dendritic calcium dynamics in deep-layer cortical pyramidal neurons. Nat Neurosci 2: 989–996.

Helmchen F, Fee MS, Tank DW, Denk W (2001). A miniature head-mounted two-photon microscope: high-resolution brain imaging in freely moving animals. Neuron 31: 903–912.

Hendel T, Mank M, Schnell B, Griesbeck O, Borst A, Reiff DF (2008). Fluorescence changes of genetic calcium indicators and OGB-1 correlated with neural activity and calcium *in vivo* and *in vitro*. J Neurosci 28: 7399–7411.

Hewapathirane DS, Dunfield D, Yen W, Chen S, Haas K (2008). *In vivo* imaging of seizure activity in a novel developmental seizure model. Exp Neurol 211: 480–488.

Higashijima S, Masino MA, Mandel G, Fetcho JR (2003). Imaging neuronal activity during zebrafish behavior with a genetically encoded calcium indicator. J Neurophysiol 90: 3986–3997.

Hirase H, Creso J, Singleton M, Bartho P, Buzsaki G (2004). Two-photon imaging of brain pericytes *in vivo* using dextran-conjugated dyes. Glia 46: 95–100.

Holtmaat A, Wilbrecht L, Knott GW, Welker E, Svoboda K (2006). Experience-dependent and cell-type-specific spine growth in the neocortex. Nature 441: 979–983.

Holtmaat A, Bonhoeffer T, Chow DK, Chuckowree J, De Paola V, Hofer SB *et al.* (2009). Long-term, high-resolution imaging in the mouse neocortex through a chronic cranial window. Nat Protoc 4: 1128–1144.

Homma R, Baker BJ, Jin L, Garaschuk O, Konnerth A, Cohen LB *et al.* (2009). Wide-field and two-photon imaging of brain activity with voltage- and calcium-sensitive dyes. Methods Mol Biol 489: 43–79.

Hoogland TM, Kuhn B, Gobel W, Huang W, Nakai J, Helmchen F *et al.* (2009). Radially expanding transglial calcium waves in the intact cerebellum. Proc Natl Acad Sci U S A 106: 3496–3501.

Hua JY, Smear MC, Baier H, Smith SJ (2005). Regulation of axon growth *in vivo* by activity-based competition. Nature 434: 1022–1026.

Illarionov BA, Bondar VS, Illarionova VA, Vysotski ES (1995). Sequence of the cDNA encoding the Ca(2+)-activated photoprotein obelin from the hydroid polyp Obelia longissima. Gene 153: 273–274.

Invitrogen. Calcium indicators. http://probes.invitrogen.com/handbook/tables/0355.html.

Jain PT, Chang SH, Gutry PP, Berezesky IK, Trump BF (1993). The relationship between [Ca2+]i and cell death using an *in vivo* model: a study using the ced-1 mutant strain of *C. elegans*. Toxicol Pathol 21: 572–583.

Jobsis FF, O'Connor MJ (1966). Calcium release and reabsorption in the sartorius muscle of the toad. Biochem Biophys Res Commun 25: 246–252.

Kao JP, Harootunian AT, Tsien RY (1989). Photochemically generated cytosolic calcium pulses and their detection by fluo-3. J Biol Chem 264: 8179–8184.

Karunanithi S, Georgiou J, Charlton MP, Atwood HL (1997). Imaging of calcium in *Drosophila* larval motor nerve terminals. J Neurophysiol 78: 3465–3467.

Kerr R, Lev-Ram V, Baird G, Vincent P, Tsien RY, Schafer WR (2000). Optical imaging of calcium transients in neurons and pharyngeal muscle of *C. elegans*. Neuron 26: 583–594.

Kerr JN, Greenberg D, Helmchen F (2005). Imaging input and output of neocortical networks *in vivo*. Proc Natl Acad Sci U S A 102: 14063–14068.

Kleinfeld D, Mitra PP, Helmchen F, Denk W (1998). Fluctuations and stimulus-induced changes in blood flow observed in individual capillaries in layers 2 through 4 of rat neocortex. Proc Natl Acad Sci U S A 95: 15741–15746.

Knight MR, Campbell AK, Smith SM, Trewavas AJ (1991). Transgenic plant aequorin reports the effects of touch and cold-shock and elicitors on cytoplasmic calcium. Nature 352: 524–526.

Knight H, Trewavas AJ, Knight MR (1996). Cold calcium signaling in Arabidopsis involves two cellular pools and a change in calcium signature after acclimation. Plant Cell 8: 489–503.

Knopfel T, Diez-Garcia J, Akemann W (2006). Optical probing of neuronal circuit dynamics: genetically encoded versus classical fluorescent sensors. Trends Neurosci 29: 160–166.

Komiyama T, Sato TR, O'Connor DH, Zhang YX, Huber D, Hooks BM *et al.* (2010). Learning-related fine-scale specificity imaged in motor cortex circuits of behaving mice. Nature 464: 1182–1188.

Kotlikoff MI (2007). Genetically encoded Ca2+ indicators: using genetics and molecular design to understand complex physiology. J Physiol 578: 55–67.

Kreitzer AC, Gee KR, Archer EA, Regehr WG (2000). Monitoring presynaptic calcium dynamics in projection fibers by *in vivo* loading of a novel calcium indicator. Neuron 27: 25–32.

Kuchibhotla KV, Lattarulo CR, Hyman BT, Bacskai BJ (2009). Synchronous hyperactivity and intercellular calcium waves in astrocytes in Alzheimer mice. Science 323: 1211–1215.

Liu HT, Gao F, Cui SJ, Han JL, Sun DY, Zhou RG (2006). Primary evidence for involvement of IP3 in heat-shock signal transduction in Arabidopsis. Cell Res 16: 394–400.

Lutcke H, Murayama M, Hahn T, Margolis DJ, Astori S, Zum Alten Borgloh SM *et al*. (2010). Optical recording of neuronal activity with a genetically-encoded calcium indicator in anesthetized and freely moving mice. Front Neural Circuits 4: 399.

Mank M, Reiff DF, Heim N, Friedrich MW, Borst A, Griesbeck O (2006). A FRET-based calcium biosensor with fast signal kinetics and high fluorescence change. Biophys J 90: 1790–1796.

Mank M, Santos AF, Direnberger S, Mrsic-Flogel TD, Hofer SB, Stein V *et al*. (2008). A genetically encoded calcium indicator for chronic *in vivo* two-photon imaging. Nat Methods 5: 805–811.

Martin JR (2008). *In vivo* brain imaging: fluorescence or bioluminescence, which to choose? J Neurogenet 22: 285–307.

Martin JR, Rogers KL, Chagneau C, Brulet P (2007). *In vivo* bioluminescence imaging of Ca signalling in the brain of *Drosophila*. PLoS One 2: e275.

Meyer-Luehmann M, Spires-Jones TL, Prada C, Garcia-Alloza M, de Calignon A, Rozkalne A *et al*. (2008). Rapid appearance and local toxicity of amyloid-beta plaques in a mouse model of Alzheimer's disease. Nature 451: 720–724.

Miledi R, Parker I, Schalow G (1977). Measurement of calcium transients in frog muscle by the use of arsenazo III. Proc R Soc Lond B Biol Sci 198: 201–210.

Miret JJ, Zhang J, Min H, Lewis K, Roth M, Charlton M *et al*. (2005). Multiplexed G-protein-coupled receptor Ca2+ flux assays for high-throughput screening. J Biomol Screen 10: 780–787.

Miyawaki A, Liopis J, Helm R, McCaffery JM, Adams JA, Ikurai M *et al*. (1997). Fluorescent indicators for Ca^{2+} based on green fluorescent protiens and calmodulin. Nature 388: 882–887.

Miyawaki A, Griesbeck O, Heim R, Tsien RY (1999). Dynamic and quantitative Ca2+ measurements using improved cameleons. Proc Natl Acad Sci U S A 96: 2135–2140.

Mostany R, Portera-Cailliau C (2008). A method for 2-photon imaging of blood flow in the neocortex through a cranial window. J Vis Exp 12: 678–679.

Murayama M, Larkum ME (2009). *In vivo* dendritic calcium imaging with a fiberoptic periscope system. Nat Protoc 4: 1551–1559.

Murphy TH, Li P, Betts K, Liu R (2008). Two-photon imaging of stroke onset in vivo reveals that NMDA-receptor independent ischemic depolarization is the major cause of rapid reversible damage to dendrites and spines. J Neurosci 28: 1756–1772.

Nagai T, Sawano A, Park ES, Miyawaki A (2001). Circularly permuted green fluorescent proteins engineered to sense Ca2+. Proc Natl Acad Sci U S A 98: 3197–3202.

Nagai T, Yamada S, Tominaga T, Ichikawa M, Miyawaki A (2004). Expanded dynamic range of fluorescent indicators for Ca(2+) by circularly permuted yellow fluorescent proteins. Proc Natl Acad Sci U S A 101: 10554–10559.

Nagayama S, Zeng S, Xiong W, Fletcher ML, Masurkar AV, Davis DJ *et al*. (2007). In vivo simultaneous tracing and Ca(2+) imaging of local neuronal circuits. Neuron 53: 789–803.

Nakai J, Ohkura M, Imoto K (2001). A high signal-to-noise Ca(2+) probe composed of a single green fluorescent protein. Nat Biotechnol 19: 137–141.

Nguyen QT, Callamaras N, Hsieh C, Parker I (2001). Construction of a two-photon microscope for video-rate Ca(2+) imaging. Cell Calcium 30: 383–393.

Niell CM, Smith SJ (2005). Functional imaging reveals rapid development of visual response properties in the zebrafish tectum. Neuron 45: 941–951.

Nimmerjahn A, Kirchhoff F, Kerr JN, Helmchen F (2004). Sulforhodamine 101 as a specific marker of astroglia in the neocortex in vivo. Nat Methods 1: 31–37.

O'Connor DH, Clack NG, Huber D, Komiyama T, Myers EW, Svoboda K (2010). Vibrissa-based object localization in head-fixed mice. J Neurosci 30: 1947–1967.

O'Donovan MJ, Ho S, Sholomenko G, Yee W (1993). Real-time imaging of neurons retrogradely and anterogradely labelled with calcium-sensitive dyes. J Neurosci Methods 46: 91–106.

Ohki K, Chung S, Kara P, Hubener M, Bonhoeffer T, Reid RC (2006). Highly ordered arrangement of single neurons in orientation pinwheels. Nature 442: 925–928.

Oka Y, Katada S, Omura M, Suwa M, Yoshihara Y, Touhara K (2006). Odorant receptor map in the mouse olfactory bulb: in vivo sensitivity and specificity of receptor-defined glomeruli. Neuron 52: 857–869.

Paredes RM, Etzler JC, Watts LT, Zheng W, Lechleiter JD (2008). Chemical calcium indicators. Methods 46: 143–151.

Park MK, Tepikin AV, Petersen OH (2002). What can we learn about cell signalling by combining optical imaging and patch clamp techniques? Pflugers Arch 444: 305–316.

Petreanu L, Mao T, Sternson SM, Svoboda K (2009). The subcellular organization of neocortical excitatory connections. Nature 457: 1142–1145.

Plieth C (2001). Plant calcium signaling and monitoring: pros and cons and recent experimental approaches. Protoplasma 218: 1–23.

Pologruto TA, Yasuda R, Svoboda K (2004). Monitoring neural activity and [Ca2+] with genetically encoded Ca2+ indicators. J Neurosci 24: 9572–9579.

Porter JT, McCarthy KD (1995). GFAP-positive hippocampal astrocytes *in situ* respond to glutamatergic neuroligands with increases in $[Ca^{2+}]_i$. Glia 13: 101–112.

Pozzan T, Rudolf R (2009). Measurements of mitochondrial calcium *in vivo*. Biochim Biophys Acta 1787: 1317–1323.

Prorok J, Kovacs PP, Kristof AA, Nagy N, Tombacz D, Toth JS *et al*. (2009). Herpesvirus-mediated delivery of a genetically encoded fluorescent Ca(2+) sensor to canine cardiomyocytes. J Biomed Biotechnol 2009: 1–12.

Reiff DF, Ihring A, Guerrero G, Isacoff EY, Joesch M, Nakai J *et al*. (2005). *In vivo* performance of genetically encoded indicators of neural activity in flies. J Neurosci 25: 4766–4778.

Ringer S (1883). A further contribution regarding the influence of the different constituents of the blood on the contraction of the heart. J Physiol 4: 29–42.

Ritter DA, Bhatt DH, Fetcho JR (2001). *In vivo* imaging of zebrafish reveals differences in the spinal networks for escape and swimming movements. J Neurosci 21: 8956–8965.

Robert V, Gurlini P, Tosello V, Nagai T, Miyawaki A, Di Lisa F *et al*. (2001). Beat-to-beat oscillations of mitochondrial [Ca2+] in cardiac cells. EMBO J 20: 4998–5007.

Rochefort NL, Jia H, Konnerth A (2008). Calcium imaging in the living brain: prospects for molecular medicine. Trends Mol Med 14: 389–399.

Rogers KL, Stinnakre J, Agulhon C, Jublot D, Shorte SL, Kremer EJ *et al*. (2005). Visualization of local Ca2+ dynamics with genetically encoded bioluminescent reporters. Eur J Neurosci 21: 597–610.

Rogers KL, Martin JR, Renaud O, Karplus E, Nicola MA, Nguyen M *et al*. (2008). Electron-multiplying charge-coupled detector-based bioluminescence recording of single-cell Ca2+. J Biomed Opt 13: 031211-1-031211-10.

Roncali E, Savinaud M, Levrey O, Rogers KL, Maitrejean S, Tavitian B (2008). New device for real-time bioluminescence imaging in moving rodents. J Biomed Opt 13: 054035-1-034035-10.

Rozsa B, Katona G, Vizi ES, Varallyay Z, Saghy A, Valenta L *et al*. (2007). Random access three-dimensional two-photon microscopy. Appl Opt 46: 1860–1865.

Russell JT, Martonosi AN (1978). The influence of pH on the absorption spectrum of arsenazo III. Biochim Biophys Acta 544: 418–429.

Salome R, Kremer Y, Dieudonne S, Leger JF, Krichevsky O, Wyart C *et al*. (2006). Ultrafast random-access scanning in two-photon microscopy using acousto-optic deflectors. J Neurosci Methods 154: 161–174.

Sato TR, Svoboda K (2010). The functional properties of barrel cortex neurons projecting to the primary motor cortex. J Neurosci 30: 4256–4260.

Schwartz TH, Bonhoeffer T (2001). *In vivo* optical mapping of epileptic foci and surround inhibition in ferret cerebral cortex. Nat Med 7: 1063–1067.

Seelig JD, Chiappe ME, Lott GK, Dutta A, Osborne JE, Reiser MB *et al*. (2010). Two-photon calcium imaging from head-fixed *Drosophila* during optomotor walking behavior. Nat Methods 7: 535–540.

Shimomura O, Inouye S, Musicki B, Kishi Y (1990). Recombinant aequorin and recombinant semi-synthetic aequorins. Cellular Ca2+ ion indicators. Biochem J 270: 309–312.

Shimomura O, Johnson FH, Saiga Y (1962). Extraction, purification and properties of aequorin, a bioluminescent protein from the luminous hydromedusan, Aequorea. J Cell Comp Physiol 59: 223–239.

Shimomura O, Musicki B, Kishi Y, Inouye S (1993). Light-emitting properties of recombinant semi-synthetic aequorins and recombinant fluorescein-conjugated aequorin for measuring cellular calcium. Cell Calcium 14: 373–378.

Shimozono S, Fukano T, Kimura KD, Mori I, Kirino Y, Miyawaki A (2004). Slow Ca2+ dynamics in pharyngeal muscles in *Caenorhabditis elegans* during fast pumping. EMBO Rep 5: 521–526.

Shummers J, Yu H, Sur M (2008). Tuned responses of astrocytes and their influence on hemodynamic signals in the visual cortex. Science 320: 1638–1643.

Sobel EC, Tank DW (1994). *In vivo* Ca2+ dynamics in a cricket auditory neuron: an example of chemical computation. Science 263: 823–826.

Stosiek C, Garaschuk O, Holthoff K, Konnerth A (2003). *In vivo* two-photon calcium imaging of neuronal networks. Proc Natl Acad Sci U S A 100: 7319–7324.

Svoboda K, Helmchen F, Denk W, Tank DW (1999). Spread of dendritic excitation in layer 2/3 pyramidal neurons in rat barrel cortex *in vivo*. Nat Neurosci 2: 65–73.

Tabata H, Nakajima K (2001). Efficient *in utero* gene transfer system to the developing mouse brain using electroporation: visualization of neuronal migration in the developing cortex. Neuroscience 103: 865–872.

Tabor R, Yaksi E, Weislogel JM, Friedrich RW (2004). Processing of odor mixtures in the zebrafish olfactory bulb. J Neurosci 24: 6611–6620.

Takahashi M, Narushima M, Oda Y (2002). *In vivo* imaging of functional inhibitory networks on the mauthner cell of larval zebrafish. J Neurosci 22: 3929–3938.

Takano T, Tian GF, Peng W, Lou N, Libionka W, Han X *et al*. (2006). Astrocyte-mediated control of cerebral blood flow. Nat Neurosci 9: 260–267.

Takano T, Han X, Deane R, Zlokovic B, Nedergaard M (2007). Two-photon imaging of astrocytic Ca2+ signaling and the microvasculature in experimental mice models of Alzheimer's disease. Ann N Y Acad Sci 1097: 40–50.

Tallini YN, Ohkura M, Choi BR, Ji G, Imoto K, Doran R *et al*. (2006). Imaging cellular signals in the heart *in vivo*: cardiac expression of the high-signal Ca2+ indicator GCaMP2. Proc Natl Acad Sci U S A 103: 4753–4758.

Tian GF, Azmi H, Takano T, Xu Q, Peng W, Lin J *et al*. (2005). An astrocytic basis of epilepsy. Nat Med 11: 973–981.

Tian L, Hires SA, Mao T, Huber D, Chiappe ME, Chalasani SH *et al*. (2009). Imaging neural activity in worms, flies and mice with improved GCaMP calcium indicators. Nat Methods 6: 875–881.

Tsesmeli N, Coumaros D (2009). Review of endoscopic devices for weight reduction: old and new balloons and implantable prostheses. Endoscopy 41: 1082–1089.

Tsien RY (1980). New calcium indicators and buffers with high selectivity against magnesium and protons: design, synthesis, and properties of prototype structures. Biochemistry 19: 2396–2404.

Tsien RY (1981). A non-disruptive technique for loading calcium buffers and indicators into cells. Nature 290: 527–528.

Tsien RY (1998). The green fluorescent protein. Annu Rev Biochem 67: 509–544.

Tsien RY, Pozzan T, Rink TJ (1982). Calcium homeostasis in intact lymphocytes: cytoplasmic free calcium monitored with a new, intracellularly trapped fluorescent indicator. J Cell Biol 94: 325–334.

Tsuruwaka Y, Konishi T, Miyawaki A, Takagi M (2007). Real-time monitoring of dynamic intracellular Ca(2+) movement during early embryogenesis through expression of yellow cameleon. Zebrafish 4: 253–260.

Wachowiak M, Cohen LB, Zochowski MR (2002). Distributed and concentration-invariant spatial representations of odorants by receptor neuron input to the turtle olfactory bulb. J Neurophysiol 87: 1035–1045.

Wachowiak M, Denk W, Friedrich RW (2004). Functional organization of sensory input to the olfactory bulb glomerulus analyzed by two-photon calcium imaging. Proc Natl Acad Sci U S A 101: 9097–9102.

Wallace DJ, Meyer zum Alten Borgloh S, Astori S, Yang Y, Bausen M, Kugler S *et al*. (2008). Single-spike detection in vitro and in vivo with a genetic Ca2+ sensor. Nat Methods 5: 797–804.

Wang JW, Wong AM, Flores J, Vosshall LB, Axel R (2003). Two-photon calcium imaging reveals an odor-evoked map of activity in the fly brain. Cell 112: 271–282.

Wang X, Lou N, Xu Q, Tian GF, Peng WG, Han X *et al*. (2006). Astrocytic Ca2+ signaling evoked by sensory stimulation *in vivo*. Nat Neurosci 9: 816–823.

Winship IR, Plaa N, Murphy TH (2007). Rapid astrocyte calcium signals correlate with neuronal activity and onset of the hemodynamic response *in vivo*. J Neurosci 27: 6268–6272.

Wong F, Fan L, Wells S, Hartley R, Mackenzie FE, Oyebode O *et al*. (2009). Axonal and neuromuscular synaptic phenotypes in Wld(S), SOD1(G93A) and ostes mutant mice identified by fiber-optic confocal microendoscopy. Mol Cell Neurosci 42: 296–307.

Yaksi E, Judkewitz B, Friedrich RW (2007). Topological reorganization of odor representations in the olfactory bulb. PLoS Biol 5: e178.

Zhang S, Murphy TH (2007). Imaging the impact of cortical microcirculation on synaptic structure and sensory-evoked hemodynamic responses in vivo. PLoS Biol 5: e119.

Zimprich F, Ashworth R, Bolsover S (1998). Real-time measurements of calcium dynamics in neurons developing in situ within zebrafish embryos. Pflugers Arch 436: 489–493.